(2)

ARL-TR-34 AR-008-346

AD-A271 331

DEPARTMENT OF DEFENCE

DEFENCE SCIENCE AND TECHNOLOGY ORGANISATION

AERONAUTICAL RESEARCH LABORATORY

MELBOURNE, VICTORIA

DTIC
ELECTE
OCT 2 0 1993
S A D

Technical Report 34

AN ASSESSMENT OF COMSCAN, A COMPTON BACKSCATTER IMAGING CAMERA, FOR THE ONE-SIDED NON-DESTRUCTIVE INSPECTION OF AEROSPACE COMPONENTS

This document has been approved for public release and sale; its distribution is unlimited

by

L. SPONDER

"Original contains color plates: All DTIC reproductions will be in black and white"

93-24721

Approved for public release.

© COMMONWEALTH OF AUSTRALIA 1993

JULY 1993

93 10 18 019

Best
Available
Copy

This work is copyright. Apart from any use as permitted under the Copyright Act 1968, no part may be reproduced by any process without prior written permission from the Australian Government Publishing Services. Requests and enquiries concerning reproduction and rights should be addressed to the Manager, Commonwealth Information Services, Australian Government Publishing Services, GPO Box 84, Canberra ACT 2601.

DISCLAIMER NOTICE

THIS DOCUMENT IS BEST QUALITY AVAILABLE. THE COPY FURNISHED TO DTIC CONTAINED A SIGNIFICANT NUMBER OF COLOR PAGES WHICH DO NOT REPRODUCE LEGIBLY ON BLACK AND WHITE MICROFICHE.

AR-008-346

DEPARTMENT OF DEFENCE
DEFENCE SCIENCE AND TECHNOLOGY ORGANISATION
AERONAUTICAL RESEARCH LABORATORY

Technical Report 34

AN ASSESSMENT OF COMSCAN, A COMPTON BACKSCATTER IMAGING CAMERA, FOR THE ONE-SIDED NON-DESTRUCTIVE INSPECTION OF AEROSPACE COMPONENTS

by

L. SPONDER

SUMMARY

This report presents some results obtained using a Compton backscatter imaging camera, developed by Philips Industries, which were obtained during a visit to the Defense Research Establishment Pacific (DREP) during May/June 1992. Compton backscatter imaging is an X-ray technique which can be used to non-destructively inspect the interior of both metallic and non-metallic structures and, unlike conventional X-ray methods, requires access to only one side of the part being inspected.

© COMMONWEALTH OF AUSTRALIA 1993

Accesion For
NTIS CRA&I
DTIC TAB
Unannounced
Justification
By
Distribution /
Availability
Dist | Avail and / or Special
A-1

POSTAL ADDRESS: **Director, Aeronautical Research Laboratory**
506 Lorimer Street, Fishermens Bend, 3207
Victoria, Australia.

DTIC QUALITY INSPECTED 2

TABLE OF CONTENTS

1. INTRODUCTION

An official overseas visit was made to Canada and the USA for a period of 25 days from May 18, 1992. This visit was co-sponsored by CRC-AS[1] and DSTO-ARL[2]. The purpose of the visit was to :-

Gain first hand experience with COMSCAN (COMpton SCANner), a commercial X-ray backscatter imaging system[3], to allow the CRC and ARL to assess COMSCAN'S capability for detecting a variety of defects in fibre composite and honeycomb materials.

Determine directions for future research into the method of Compton backscatter imaging by CRC/ARL and the possible future collaboration between ARL and Defence Research Establishment Pacific (DREP).

Discuss the experiences of the Boeing Commercial Aircraft Company toward COMSCAN and Compton backscatter imaging, in general, for their purposes and to assess their level of research/development into the technique.

Fourteen working days were spent in the Nondestructive Evaluation Group of the Materials Technology Section at the Defense Research Establishment Pacific (DREP) where the COMSCAN imaging instrument was kindly made available for the author's use.

A one day visit was subsequently made to the Boeing Aircraft Company in Renton, Seattle, to discuss their interests in Compton scatter imaging.

2. SUMMARY OF X-RAY IMAGING METHODS

2.1 Principle of Compton Scatter Imaging (CSI)

The basis of Compton scatter imaging is the detection of X-rays scattered by electrons in the target specimen (Figure 1). For materials with an atomic number up to about thirteen (Aluminium) and for X-rays in the energy range from about 80 keV to 500 keV the dominant interaction process is Compton scattering.

In the Compton process an X-ray photon interacts with an electron whose binding energy is much less than that of the photon. The result is that the X-ray scatters at an angle with a reduced energy, the energy difference being transferred to the electron as kinetic energy. The amount of scattering from a given volume element within the target depends on the number of 'free' electrons encountered which is a function of the mass density and atomic number of the scattering material. By recording the amount of scattering from different regions in the target images can be generated in which the resulting contrast is related to variation in density.

1Co-operative Research Centre - Aerospace Structures

2Defence Science and Technology Organisation - Aeronautical Research Laboratory

3Philips Electronic Instruments

2.2 Conventional X-ray Methods.

Conventional X-radiography involves the partial absorption of X-rays through the target with the imaging medium, usually film, recording the relative intensity of the transmitted beam. The result is a two dimensional (2-D) projection map of the absorption of the X-ray beam in different regions of the specimen. As a first approximation the image may be interpreted as a map of the mass density which has been integrated over the total beam path between source and detector.

An extension of the conventional radiographic process, called computed tomography (CT), uses mathematical reconstruction techniques to generate detailed three dimensional (3-D) maps of the internal structure through the part. Film recording is replaced with an array of detectors and the images are generated as a series of through-thickness slices. To acquire the information required for the reconstruction process many data sets must be recorded each at a different angle of the specimen with respect to the incident X-ray beam. CT systems typically require access to the part over a range of 180° although for the best resolution 360° rotation is desirable.

2.3 CSI versus CT

Compton scattering offers 3-D imaging comparable to CT but without requiring rotation of the part. Data can, in principle, be acquired at any desired angle with respect to the X-ray source and complex mathematical image reconstruction is not required. The time for the data collection and computer processing can, therefore, be significantly less than that required for CT work. Larger parts can be examined with Compton scattering imaging which would be difficult or impossible with the CT method. In particular, CSI offers the distinct advantage that, since the detector can be placed on the same side as the X-ray source, one-sided imaging is possible whilst retaining full 3-D imaging capability.

CT systems on the other hand are well developed and have demonstrated very high spatial resolution (~10 μm) for small specimens, although incurring a heavy time penalty for the data collection and processing. cf. the spatial resolution of CSI in the Comscan system which is of order 0.2 mm*0.2 mm*0.2 mm. CSI, however, is still relatively new and further development will likely lead to significant performance improvements.

3. COMSCAN

3.1 Hardware

A schematic of the COMSCAN system developed by Philips is shown in Figure 2. X-rays are produced by a conventional industrial X-ray tube operating at up to 160 kV and 18.75 mA (3kW total power). Line scanning and collimation of the X-rays into a pencil beam are achieved simultaneously with a novel rotating collimator system. The crossover region of helically cut slits (diamond shaped) on concentric drums generates a 'hole' or exit slit which passes, unattenuated, a portion of the fan beam produced by the X-ray tube. As the drums are rotated by a small motor the result is a flying X-ray spot (pencil beam) of dimensions about 0.5 mm*0.5 mm at the exit surface of the collimator. The complete raster pattern is generated with the aid of a motor which drives the entire camera assembly, consisting of the X-ray tube and detectors, forward at the end of each line until the required area has been scanned. The entire camera assembly consisting of the X-ray source , detectors, scanning motors and associated electronics is integrated into a single portable unit.

The data are acquired by the process illustrated in Figure 3. Two independent sets of Bismuth Germanate ($Bi_4Ge_3O_{12}$) scintillation detectors intercept the backscattered X-rays through two fixed slit collimators placed symmetrically with respect to the exit slit.

There are two banks of 11 detectors each on opposite sides of the exit slit, each detector measuring approximately 0.9 mm*2 mm*60 mm. Each detector acquires data, in the form of scattered X-ray photons, from a different depth within the specimen resulting in 22 image slices with one pass. Odd and even image slices are recorded by alternate detectors which lie on opposite sides of the exit slit.

Philips provide collimators spanning the depth ranges 5 mm, 10 mm, and 50 mm. The ability, in practice, to produce useable images at a particular depth is actually determined by the intensity of the backscattered radiation. The deeper the image slice the lower, in general, the backscatter intensity and, as a consequence of the collimator geometry, the poorer the depth resolution. The approximate thickness and depth resolution for the available collimators is given in Table 1 below.

TABLE 1

SLICE THICKNESS AND RESOLUTION FOR DIFFERENT COLLIMATORS

Collimator (mm)	Slice thickness (mm)	Depth Resolution (mm)	In-plane Resolution (mm^2)
5	0.9	0.23	0.2
10	0.9	0.45	0.2
50	0.9	2.25	0.2

The lateral resolution in the plane of the image is set by the rate at which the data is sampled. The standard rate produces square image pixels with dimensions of about 0.2 mm*0.2 mm.

3.2 Software

The software operating environment is unique to Comscan and consists of a simple set of menu driven selections that give the user basic control over parameters of the X-ray generator, scanning motors and data acquisition.

3.2.1 X-ray Generator

The X-ray tube voltage and current are both controlled through software in steps of 0.1 keV and 0.01 mA respectively. There are also two choices of spot size, standard and small, although no reference is given as to the actual dimensions or the appropriateness of the different settings for different situations. The performance of the two spot sizes were compared in one experiment but we were unable to detect a qualitative difference in the images. Consequently, all of the images in this work were recorded using the standard spot size.

3.2.2 Scan Parameters

The scan dimensions and scanning speed are controlled by software. The scan dimensions are controlled by the number of lines to a maximum of 500, corresponding to a traverse of 100 mm. The scan width is fixed at 50 mm. The number of pixels per scan line is not adjustable.

Scan speeds are calibrated in multiples of the integration time per pixel of 600 msec. There are 5 predefined scan speeds labelled 1 to 5 corresponding to integration times of 3000 msec per pixel and 600 msec per pixel respectively. At speed setting 3 the time to scan an area of 50 mm*100 mm is 6 minutes. It is possible, though inconvenient, to obtain other scan speeds beyond the standard choices. Some of the author's scans, for example, were carried out at 6000 msec per pixel ie. 1/2 of speed setting 1.

3.2.3 Image Processing and Display

The menu of available display and image processing functions as listed in the COMSCAN manual, including various filter types, is presented in Appendix 2. Images can be displayed one slice at a time or up to two at a time from arbitrary slices. In addition to contrast enhancement, color and monochrome lookup tables can be manipulated and there are also zoom/pan and scroll display functions. Addition or subtraction of grey values for the whole image is also supported.

A scan of a perfectly uniform test article will not, in general, produce images with uniform intensity. This is due to the combined effects of:-

1) Inhomogeneity of the X-ray source
2) Method of collimation
3) Differences in the sensitivities of the detectors
4) Non-uniform absorption by the target caused by variations in the total X-ray path length along a scan line.

The effect, illustrated in Figure 4, is that :-

1) the intensity varies across individual lines in an image, being highest at the center and diminishing towards the edges
2) the mean intensity may fluctuate from slice to slice and will decrease, in general, the deeper the image slice.

A calibration, known as a shading correction, can be made with the COMSCAN software but it requires that a suitable standard be available. The standard, which hopefully would have similar scattering properties to the actual target, must first be scanned to allow the software to calculate the necessary corrections and these are then applied to further scans.

At the commencement of this work a teflon block was used as the calibration standard but it was found that, for our honeycomb structures in particular, there was no significant advantage to be gained. For this reason and since the software applies the shading corrections to the raw data, and is irreversible, no such corrections were made.

The only alterations to the image data given in this report have been with respect to contrast and brightness in order to create an acceptable and consistent print quality.

3.2.4 Data Storage and retrieval.

A complete set of 22 images requires 2.8 Megabytes (22 * 128K Bytes) of digital storage. Each pixel in the image is written to memory as a 12 bit grey level (2^{12}= 4096 grey levels) but, to reduce storage overheads, the data are saved to disk using only the most significant 8 bits of each data byte. The dynamic range of the recorded information is thus reduced to 256 grey levels. To avoid truncating the pixel values during the save operation the user can choose to offset the values to fit within the allowable dynamic range before saving the data. The image data format consists of a variable length header containing file comments entered by the user, followed by row and column values representing each pixel in the image.

4. EXPERIMENTS PERFORMED AT DREP

DREP purchased a COMSCAN device in late 1991 and have since been trialing the system. Minor problems with both the software and hardware have slightly limited its use although throughout this visit the unit was functioning reliably. In the DREP system the COMSCAN assembly is mounted onto a mechanical manipulator with six degrees of freedom, consisting of three mutually orthogonal rotation and translation axes. The manipulator allows an operator to reposition the COMSCAN head for wide area scans from a remote location with minimal effort and also facilitates simpler alignment.

During the visit to DREP it was possible to apply Comscan to several test specimens.

In the images presented here dark areas correspond to a low scattered flux at the detector which may be due to either lower scattering or higher attenuation. Less scattering occurs from less dense materials and greater attenuation is caused by intervening materials of higher density.

The images were printed on a Canon colour copier/printer (model 300) which gave only a slight loss of quality when compared with the images as viewed on a video monitor capable of displaying 256 grey scales.

4.1 ARL Test Article: Panel P1

Two honeycomb composite specimens were manufactured at ARL for this work. Only the more complex of the two, designated P1, was scanned. This panel is shown in Figure 6. It is a square panel of side length 295 mm notched at one corner for easy identification of orientation. The carbon fibre sheets are each 10 plies thick (total thickness approximately 1 mm) the layup sequence being +45°, -45°, 0°, 90°, 0°, 0°, 90°, 0°, -45°, +45°. A septum divides the panel internally, one part consisting of a 1" core of nomex honeycomb and the other a dual core of 1/2" aluminium honeycomb and 1/2" nomex honeycomb placed back to back and separated by another carbon fibre sheet identical in layup to the face sheets. The surface directly above the join of the different sections is stepped owing to a slight thickness mismatch and the join line has been filled with a foaming adhesive.

Artificial defects were placed in all three skins and between the skins and honeycomb core. Figures 7 and 8 show the position and type of each defect and Table 2 gives a brief description of each. The results are described below.

4.1.1 Grid A. (Figure 12)

160 kV, 18.75 mA, speed 3, 10 mm collimator.

About 1 millilitre of water was injected into the Aluminium honeycomb using a hypodermic syringe.

Slice 10. Depth ~10.8 mm. The honeycomb only is clearly visible and there are indications of distributed water appearing as white halos lining the cell walls.

Slice 13. Depth ~14 mm. The middle carbon fibre sheet is beginning to appear as a general light background partially obscuring the water containing cells. Contrast this image with that of Figure 21 where the cells containing water have remained localized.

4.1.2 Grid D. (Figure 13)

160 kV, 18.75 mA, speed 3, 5 mm collimator.
A layer of fine glass beads, ranging in size from about 320 mm to about 450 mm, was introduced between adjacent skin plies in the middle of the sheet.

Slice 2. This image reveals surface details such as the 45° ply orientation and minor surface irregularities. The region directly over the patch appears lighter because the skin is slightly raised.

Slice 6. The honeycomb is beginning to appear and the image is brighter overall due to scattering by the carbon fibre. The glass bead layer is obscured owing to the similar scattering power of the fibre/glass combination compared with air/glass.

Slice 12. Depth~ 2.3 mm. Scattering by the glass beads is still evident. The glass beads are at a depth below the surface of about 0.5 mm and the voxel thickness is nominally about 0.9 mm. In this case the effective voxel thickness appears to be at least 1.8 mm (2.3 mm - 0.5 mm). At a depth of 3.2 mm (slice 16) the simulated defect is no longer visible.

4.1.3 Grid E. (Figure 14)

160 kV, 18.75 mA, speed 3, 5 mm collimator.

Partially overlapping circular patches of adhesive were placed between the middle plies of the carbon fibre sheet prior to curing.

Slice 6. Depth~0.5 mm. The patches are distinctly visible although the shape is indistinct. Close inspection suggests a slight density change where the individual patches overlap although this is by no means certain.

Slice 9. Depth~1.1 mm. The patches have disappeared.

4.1.4 Grid G/H. (Figure 15)

160 kV, 18.75 mA, speed 3, 10 mm collimator.

Slice 11. Depth~13 mm. Imaging the wire inserts in the middle carbon fibre sheet. The inserts in the middle sheet appear as white whereas the sharply defined dark outlines are artefacts due to absorption of the incident X-rays by the wires in the upper carbon fibre sheet. The diffuse shadows are also caused by absorption of the wires in the top sheet although in this case the absorption is of the scattered X-rays rather than the incident beam.

Slice 12. Depth~13.5 mm. Notice in this slice that the diffuse shadows have shifted their position relative to the stationary objects. Since the detectors 'see' only the scattered X-rays this effect supports the argument that these are caused by absorption in the scattered radiation rather than the incident X-rays.

Slice 17. Depth~15.8 mm. At this depth all the wires are visible only by the absorption that they cause.

4.1.5 Grid H. (Figures 16, 17)

160 kV, 18.75 mA, speed 3, 5 mm collimator.

Metal wires were bent to form loops and then embedded between the middle plies in the upper and middle carbon fibre sheets.

Slice 2. Depth~0 mm. Diffuse images near the surface of the sheet due to the surface distortion caused by the wires underneath.

Slice 5. Depth~0.7 mm. The scatter image of the wires.

Slice 8. Depth~1.4 mm. Note the dark halo at the right edges of the wires. This is caused by shadowing of the scattered radiation by the wires as seen by the detector on one side of the COMSCAN head.

Slice 9. Depth~1.6 mm. Note that the dark halos are now on the opposite side of the wires since this slice was imaged by a detector on the opposite sides of the defect. The horizontal dark halos surrounding the lower pair of wires is believed to be caused by bridging of the carbon fibre plies.

Slice 12. Depth~2.3 mm. The attenuation of the scattered radiation by the dense material of the wires is easily seen well below the wires.

4.1.6 Grid I. (Figure 18)

160 kV, 18.75 mA, speed 3, 5 mm collimator.

The honeycomb was impacted to cause crushing and the carbon fibre layup was then cured to the honeycomb. Due to the applied pressure during the cure cycle a recess was formed a in the sheet directly over the impacted core.

Slice 6. The carbon sheet is responsible for most of the scattering so that the impacted area appears dark.

Slice 12. The impacted area and the uncrushed honeycomb are both visible and there is some contribution from the carbon fibre away from the crushed core.

TABLE 2.

Defects/features in specimen P1 and their location. Defects/features which straddle more than one scan grid are superscripted. Identically numbered features refer to the same item.

Grid	Location	Defect	Defect/Feature Description	Detected by COMSCAN
A	Al honeycomb		a) Water injected into the middle of Al honeycomb b) Contaminant between skin and honeycomb[1]	Yes
B	I, II	1	Contaminant between skin and honeycomb[1]	No
C	I, II	2	Double layer of Teflon sandwiched between middle plies	No
D	I, II	3	Layer of glass beads (320μm to 450μm dia.) sandwiched between middle plies	Yes
E	I, II	4	Partially overlapping patches of adhesive	Yes
F	-	-	-	-
G	I, II	7	Wire inserts between middle plies[2] Peel Ply[3]	Yes
H	I, II	7	Wire inserts between middle plies[2]	Yes
I	I	8	Crushed Honeycomb Core	Yes
J	I, II	5	Peel Ply[3] Backing tape	No
K	I, II	9	Knife edge cuts in middle ply at 0° and 90°	No
L	-	-	-	-
M	Refer Figure 7	-	-	-
N	Refer Figure 7	-	Septum[4]	Yes
O	Refer Figure 7	-	Septum[4]	Yes
P	Nomex Honeycomb		Water injected into the middle of the Nomex honeycomb	Yes
Q	Refer Figure 7	-	Bakelite block with centre drilled hole. Foaming adhesive inserted around the periphery of the block	Core, hole and adhesive
R	I	10	1cm diameter hole drilled in the skin to the top of the honeycomb below. The hole was impacted with an oversized mandrill to induce delaminations on the periphery of the hole and the whole was finally sealed with an epoxy resin	

4.2 Hawker de Havilland Test Article: Panel P2 (Figure 22)

Panel P2 (Figure 9) is a carbon fibre composite step wedge specimen made up of woven fibre plies. The panel itself was believed to have been manufactured as a standard for ultrasonic inspection and although defects were known to exist in the panel the type of defect was unspecified. A transmission X-ray, Figure 10 (a), of the part shows a series of irregular dark patches and these are also visible as lighter areas in the COMSCAN images (Figure 22). The defects, as seen by COMSCAN, appear to be at or very close to the surface of the part. An ultrasonic C-scan over the same area is shown in Figure 10 (b), however, shows a variety of overlapping defects, probably Teflon inserts, of which the most evident is at a depth no closer than the middle of the panel.

In this case it appears that COMSCAN is detecting the defects by the consequent slight surface deformation rather than by imaging the Teflon directly. This is consistent with the fact that in the P1 test article the Teflon inserts that were embedded in carbon fibre were not visible and is in line with other DREP findings.

4.3 ASTA Test Article: Panel P3 (Figure 23)

The ASTA test article shown in Figure 11 is a section from an aircraft door consisting of carbon fibre skins enclosing a nomex honeycomb. The maximum total thickness is 60 mm. The region under the dotted line in Figure 11 has been strengthened by the insertion of a fibreglass insert. This insert, which is potted to the core, forms an attachment surface for an external hinge.

Slice 3 Depth~3mm. The bright lower half of the image is from the fibreglass insert which is surrounded by the potted honeycomb (grey). Dark spots within the grey area indicate porosity which was later confirmed by visual inspection of a cross-section of the part. At the left edge is a circular lead target used in an earlier radiographic inspection.

4.4 Miscellaneous

Figures 24 and 25 show the sensitivity of COMSCAN to surface texture. In this example we can see surface texture in the more prominent items of this set of Australian, Canadian and United States coins.

Slice 1. Obvious surface relief in this Australian coin.

Slice 2. These two coins have appeared first since they are thicker than the others.

Slice 5. The remaining coins and their surface features.

Slice 10. Notice in the coin at bottom right that the high points of the surface relief, which in slice 5 are bright have reverse contrast in this deeper slice due to absorption rather than scattering. The wood baseboard, on which these coins have been placed, is beginning to scatter as evidenced by the bright areas between the coins. The baseboard may be masking detection of the surface relief on the back surfaces of the coins.

5. BOEING COMMERCIAL AIRCRAFT COMPANY

A visit was made to the Boeing Quality Assurance Research and Development Section in Renton, Seattle.

Boeing, in a beta test agreement with Philips, have applied COMSCAN to approximately 30 test articles both composite and metal. Some of these were aircraft parts that had been in service, others were proposed structures and some were test coupons from engineering studies.

In the metal structures they found:-

Gaps under rivet heads greater than 1/8 mm and gaps in splices and doublers

Corrosion damage where the corrosion had been removed from the surface. In cases where the corrosion product was in place the detectability was lower due to the similarity of scattering by pure metal/corrosion product.

Cracks. Short cracks and/or closed cracks were not detected.

Sealant

In the composites they found:-

Excellent sensitivity to potting material and water in honeycomb

Good results verifying the presence of adhesive between the face sheet and core although they were unable to gauge the bond line thickness

Sheared core from impacts on the face sheet and delaminations within the face sheet caused by lightning strike.

Large scale porosity

Some types of bridging defects

Tunnel voids in graphite epoxy

Potting compounds were easily detected and their location and extent were quantifiable

Resin variations and ply orientation in some structures

Boeing personnel recognise that the COMSCAN system is a major technical accomplishment and that it has established the credibility of the backscatter technique for one-sided inspection. However, COMSCAN is not seen as a tool for high volume usage and coupled with the high purchase cost they do not recognise a commercial application at this time.

Boeing are continuing to develop in-house X-ray CT and Compton scattering apparatus.

6 CONCLUSIONS

The COMSCAN system, since it produces images based on mass density, is not particularly sensitive to introduced defects whose density is similar to the neighbouring material. Teflon inserts in the carbon/epoxy resin of panel P1, for example, were not visible in this work although similar defects have been detected with COMSCAN and also metallic foils in fibre reinforced plastics[3].

On the other hand COMSCAN is particularly sensitive to details of surface texture where the surface is in contact with air. Voids are readily detected, in general, and corrosion can be detected indirectly by it's effect on surface roughness.

The resolution of the COMSCAN system is limited to the size and shape of the scattering volume ('voxel) contributing to each data point which is determined by the collimator, 'tector geometry and details related to the beam profile.

The ability, in practice, to differentiate features depends on various factors including:-

1) the relative scattering powers of the contributing materials
2) the masking of features by absorption
3) noise
4) multiple scattering

Planar defects such as delaminations, in particular, can be difficult or impossible to detect particularly where these defects are embedded in a matrix of similar scattering power.

Absorption by intervening features can produce visible artefacts in images of deeper slices which can complicate the resulting images or even mask particular features so that a high degree of interpretive skill is required.

The ability to detect and recognize particular defects relies on the user's ability to differentiate contrast differences and make judgements based on them. These differences may be slight and can be significantly affected by intervening materials/objects along the X-ray beam path. Images also tend to be quite noisy as a consequence of low count rates so that it is possible for the user to overlook or misinterpret features particularly when a priori information about the nominal structure is not available. The application of image processing techniques could significantly improve the detectability of subtle features.

7. ACKNOWLEDGMENTS

The author wishes to thank Dr. Gordon Long, as head of the CRC-AS, for making this work possible and for his advice and encouragement.

My sincere appreciation to the 'gang' in the Nondestructive Evaluation Group at DREP for their many efforts on my behalf and especially for their hospitality. In particular I wish to thank Dr. W. Sturrock for making the DREP facilities available to me and to R. Finlayson for his friendship and for giving up his time to support this work.

I would also like to thank Dr. S. Burke (ARL) for his advice during the preparation of this report and W.Waldman (ARL) for his assistance with the retrieval of the image data.

APPENDIX 1:

COMSCAN APPLICATION REPORTS

Philips have produced a set of inspection reports using COMSCAN which give results for particular applications and with various materials and defects. These are available to potential customers upon request. Some of these reports which were available to the author at DREP are listed below.

[1]. **A COMSCAN Investigation of Glass Reinforced Plastic / Foam Sandwich Material.** K.K. Yeung, P. Lambrineas, R.D. Finlayson, W.R. Sturrock, B. Suendermann and J.R. Davis.

[2]. **Non Destructive Testing of a Laminated Aircraft Door with the COMSCAN Method.** Philips International Product Group, Hamburg.

[3]. **Non Destructive Testing of Fibre Reinforced Plastics with the COMSCAN System.** Harding, G. and Fischer, K.H. Philips, Hamburg.

[4]. **Detection of Water and Moisture Ingress of Honeycombs.** Philips International Product Group, Hamburg.

[5]. **COMSCAN. The New Non-destructive Inspection Technique for Fibre Reinforced Composite and Light Alloys.** Roye, W. Conference paper presented at NDT '91, August 19-21 1991, World Congress Centre, Melbourne.

APPENDIX 2:

COMSCAN MENUS

Two of the menus listed in the COMSCAN manual.Filter Menu

Filter Menu

average
sharp1
sharp2
V-edge
H-edge
Laplace1
Laplace2

Imaging Menu

	1- show single layers
	2 - display of two layers
	3 - subtract layers
	4 - lut
	5 - zoom/pan and scroll
Display Functions:	6 - image comment
	7 - mark area
	8 - reset display
	9 - standard video
	10 - no overlay
Image processing:	11 - low-pass

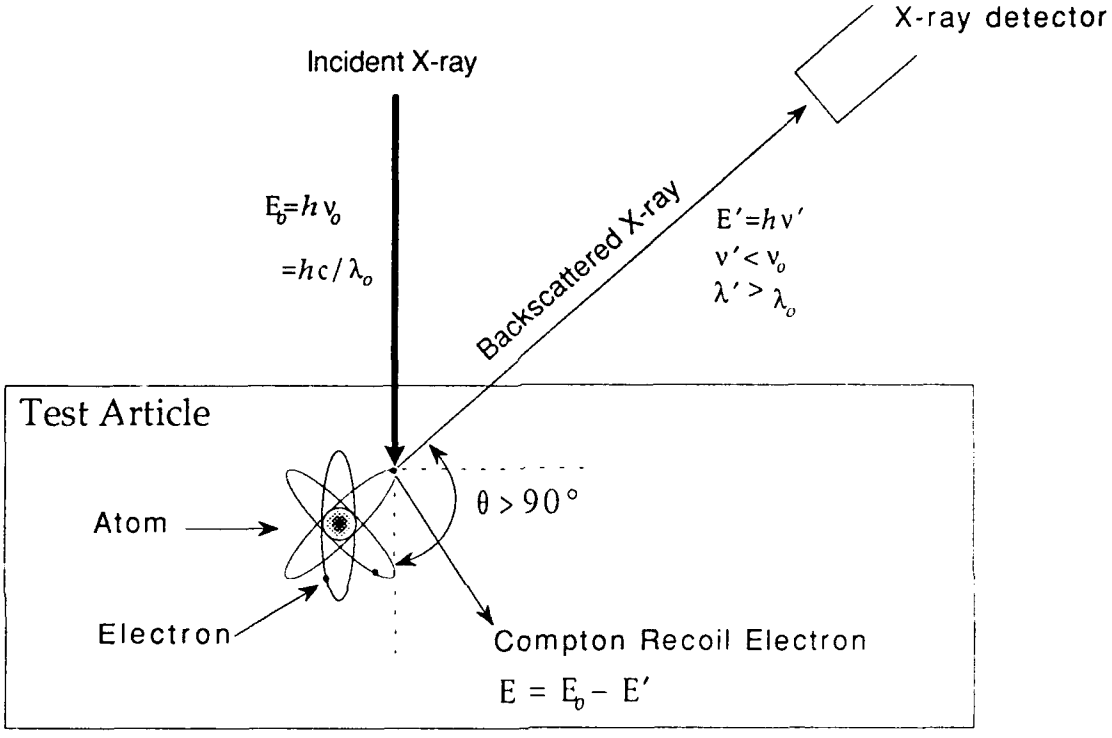

Figure 1. The Compton backscatter process. An X-ray photon of energy, E_o, scatters from an atomic electron with reduced energy, E'.

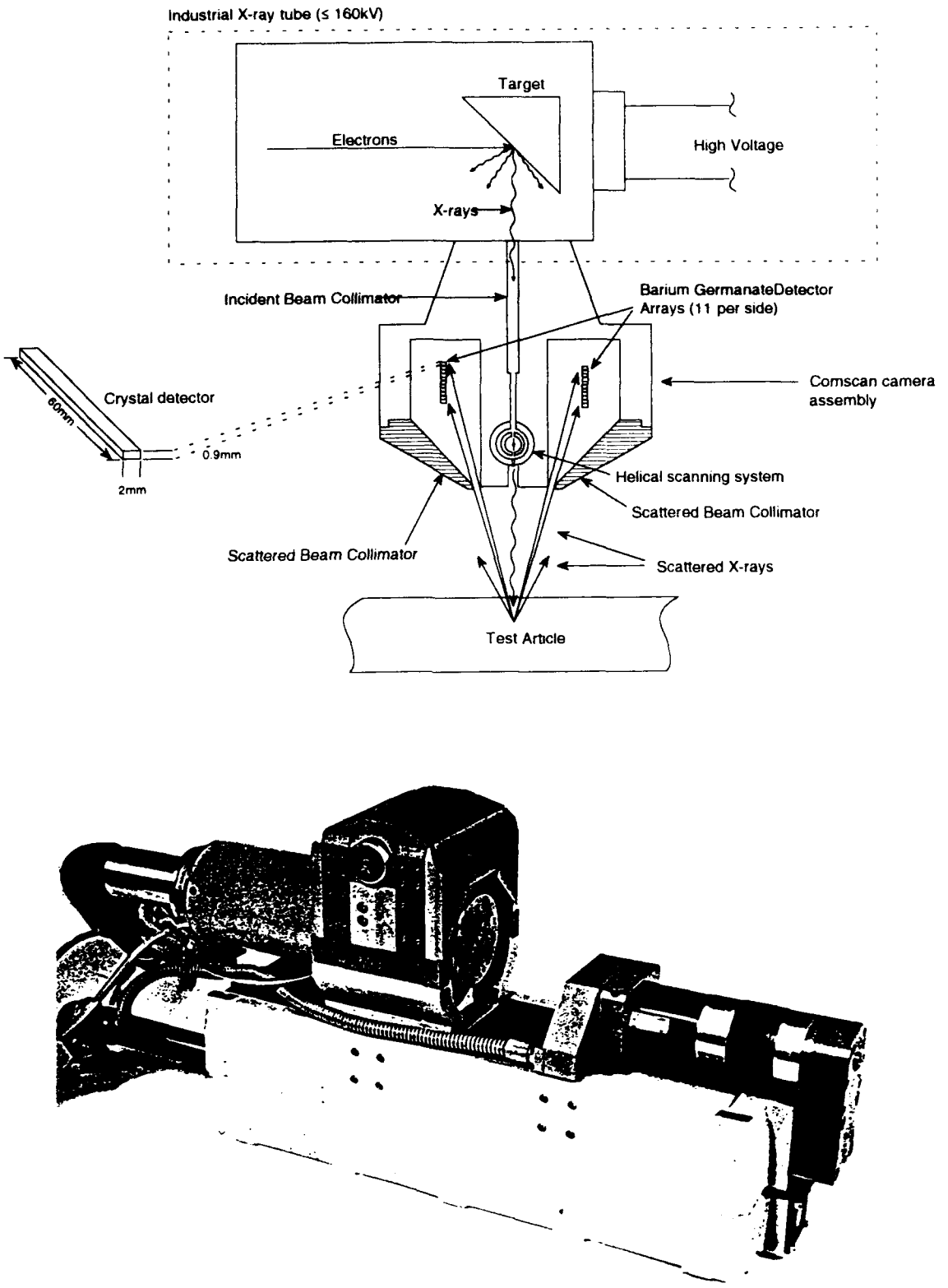

Figure 2. X-ray Source and Detector Geometry

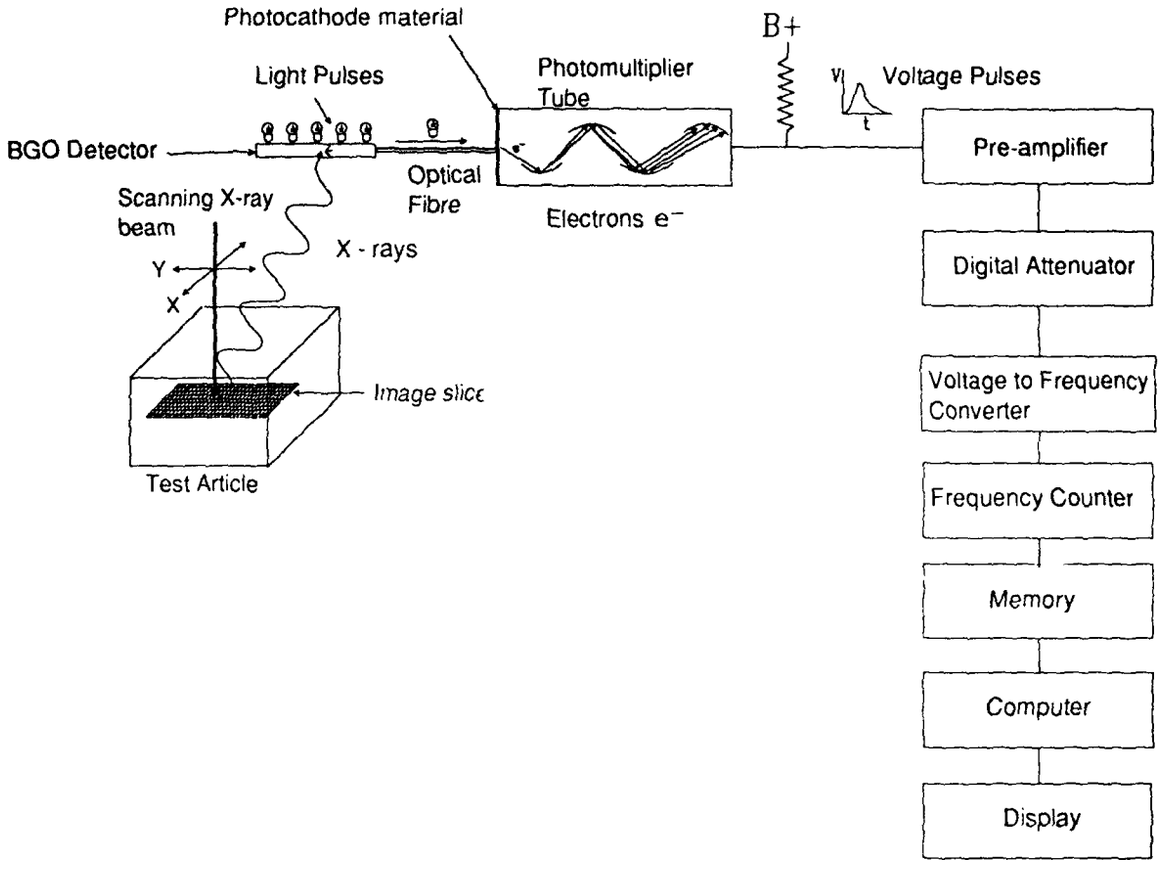

Figure 3. Basic components of the Comscan System.

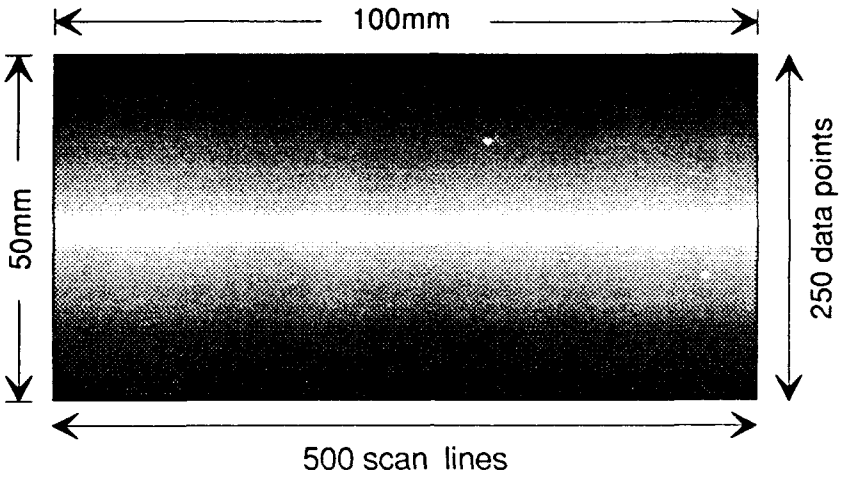

Data storage per scan = 500 * 250 * 8bits
= 125000 Bytes

Pixel dimensions = 0.2mm * 0.2mm

Figure 4. Scan details and the shading effect.
At each position of the scanner the pencil beam traverses the width of the scan area to give 250 data points (pixels) per line. On completion of a scan line the head moves to the next line and the process is repeated until all 500 lines are scanned. The effect known as shading on a nominally uniform test article is represented by the shading shown here.

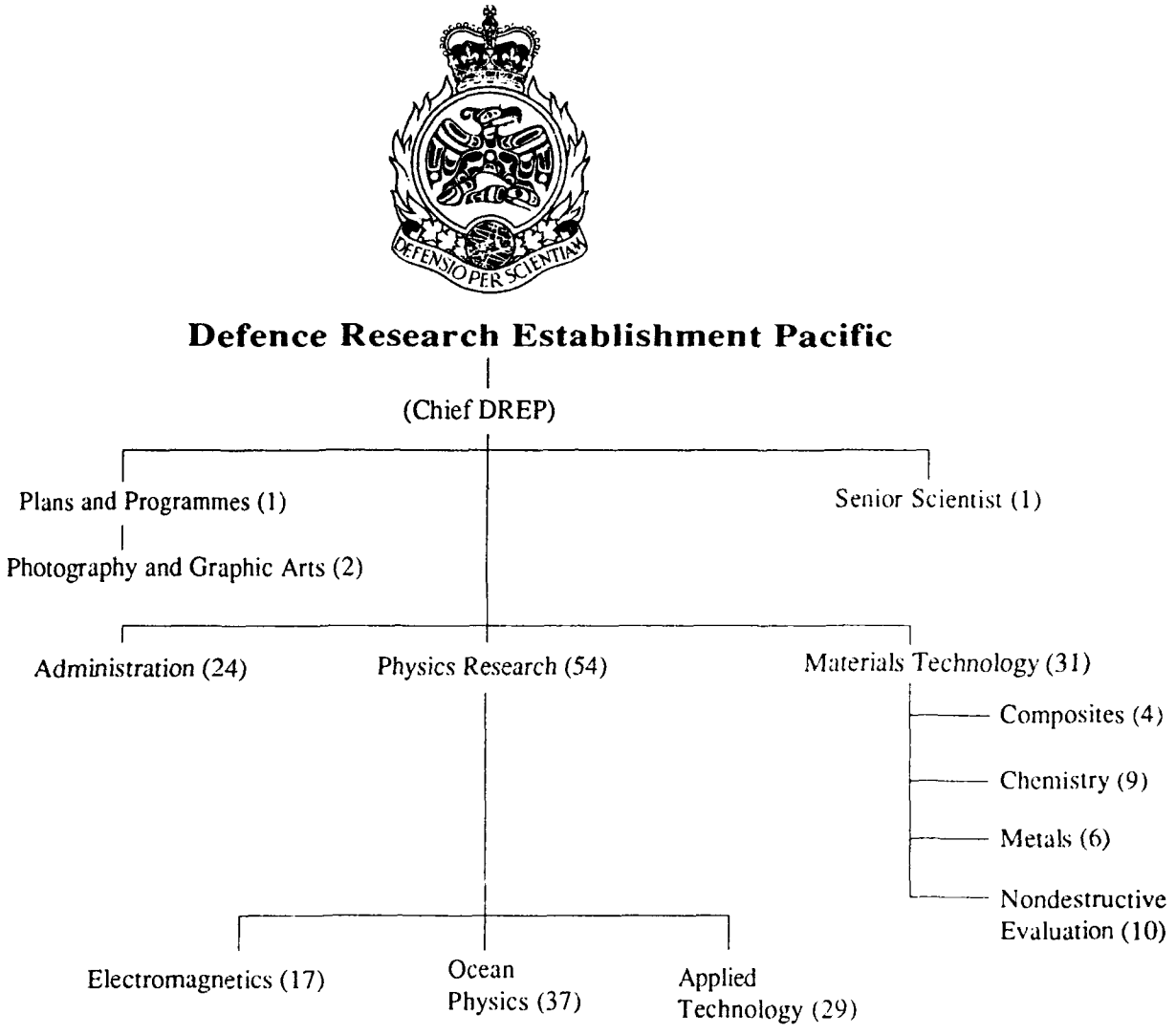

Figure 5. The DREP Internal Structure Numbers in parenthesis are staff numbers.

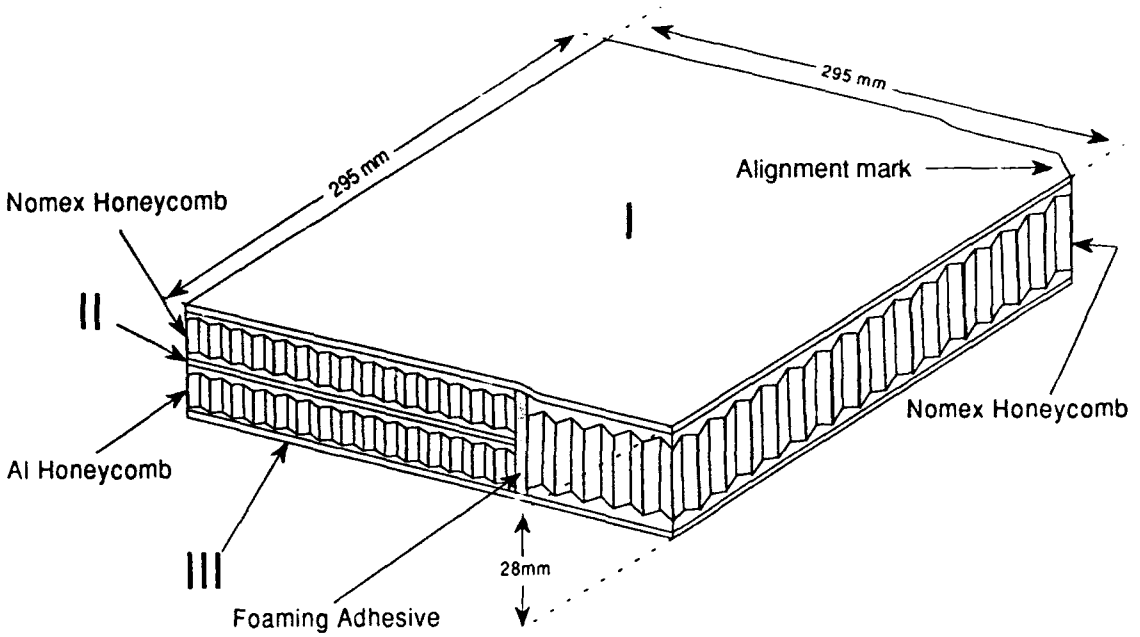

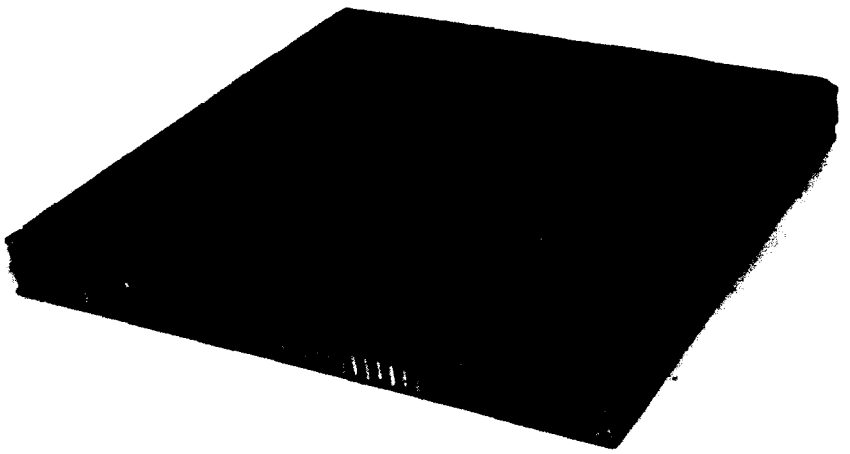

Figure 6. Specimen P1.

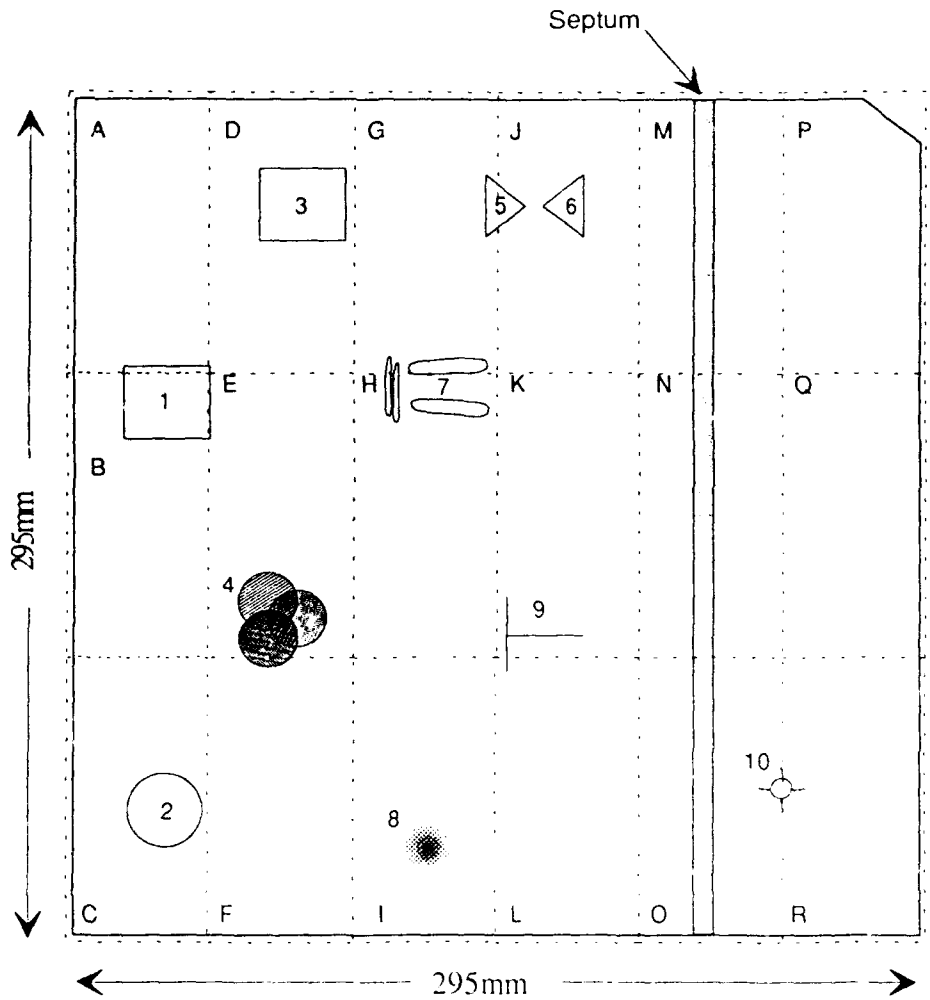

Figure 7. Plan view of specimen P1 showing implanted defects/features in the upper (I) and middle (II) composite skins. The dashed lines denote boundaries of individual scan areas and numbers are used to specify individual features.

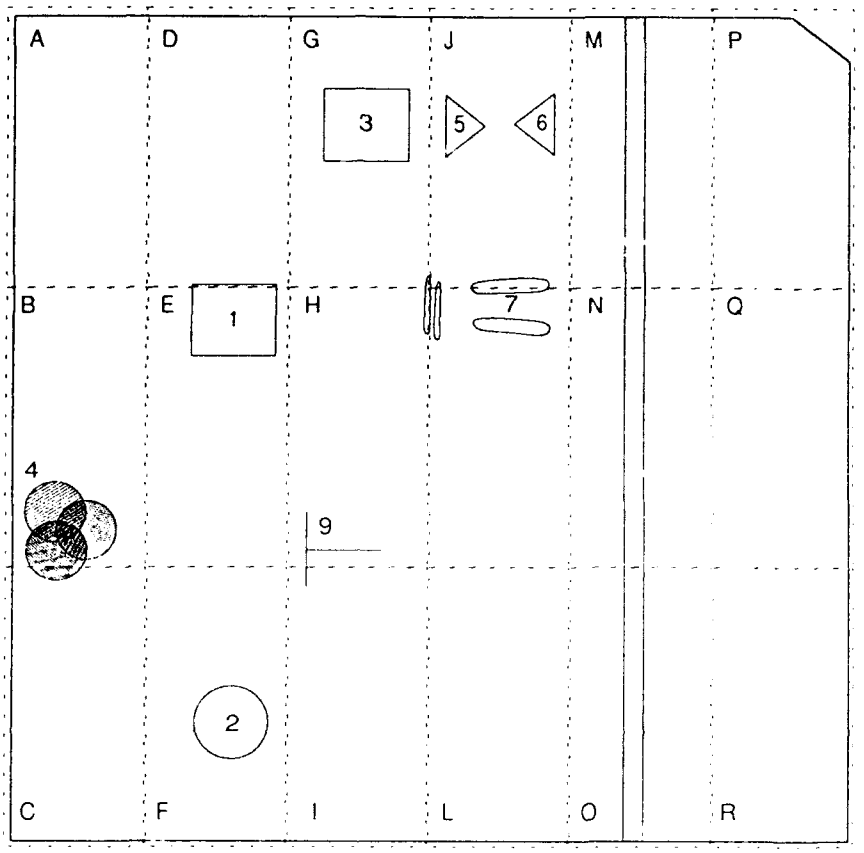

Figure 8. Plan view of specimen P1 showing implanted defects/features and their position in the lower (III) composite skin.

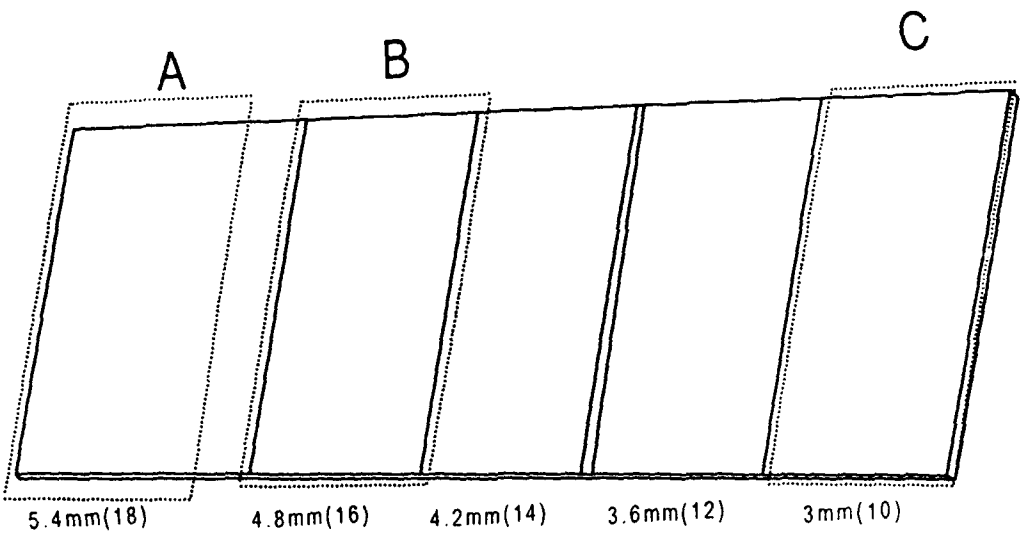

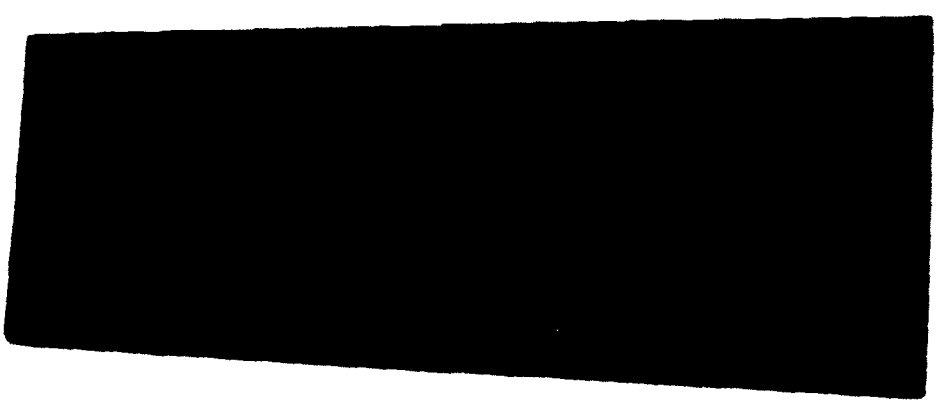

Figure 9. Step wedge specimen P2. Dotted areas refer to sections which were scanned (refer to text) and the numbers in parentheses refer to the part thickness in plies.

(a)

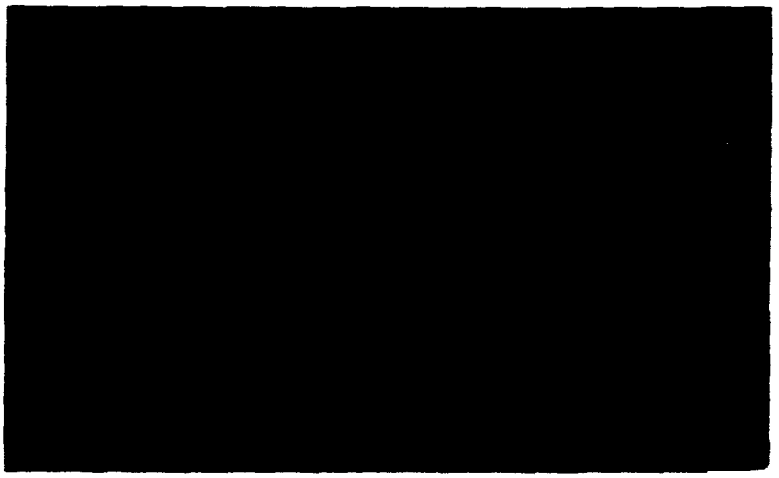

(b)

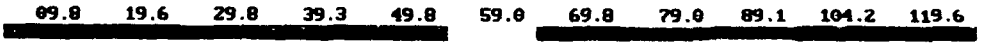

Figure 10. Panel 2. (a) Transmission X-ray through grid B of panel P2 revealing unspecified defects, probably Teflon inserts (see text). (b) Ultrasonic C-scan of the same section using a 2.25MHz probe. The colours represent the time-of-flight of the return pulse (echo) as a percentage of the total thickness of the whole part. Violet (104.2%) represents the echo from the back face of grid B.

(a)

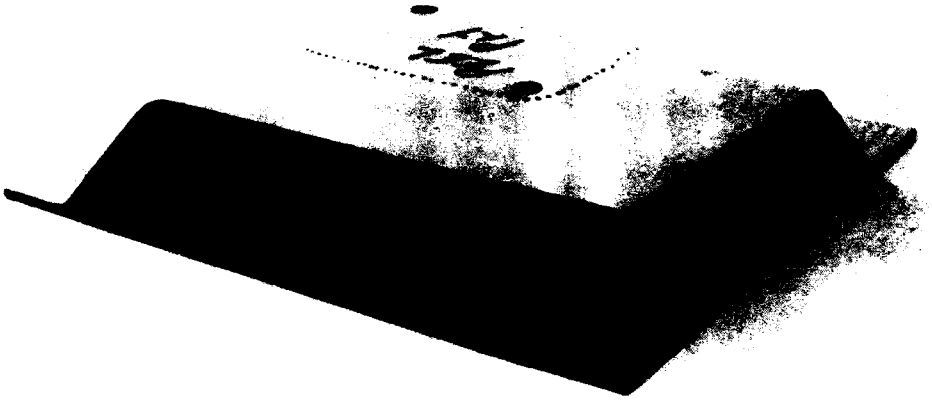

(b)

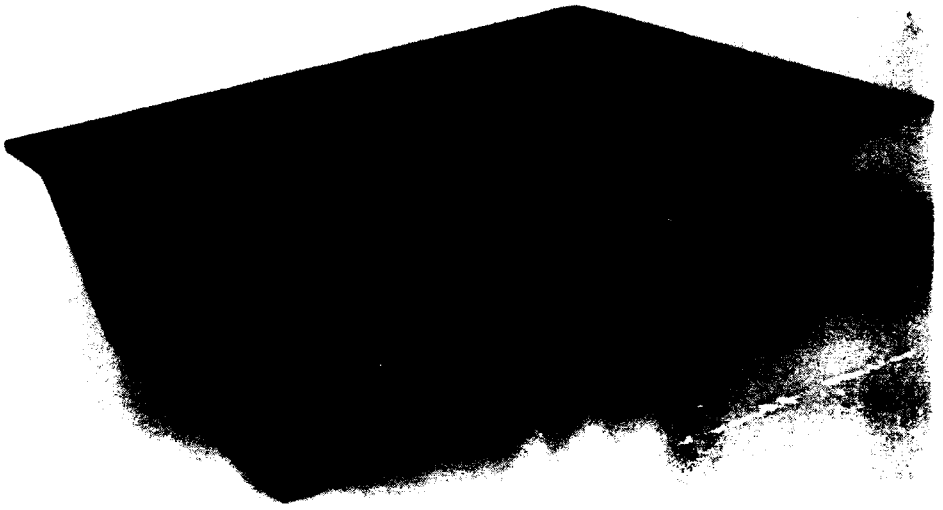

Figure 11. Specimen P3.

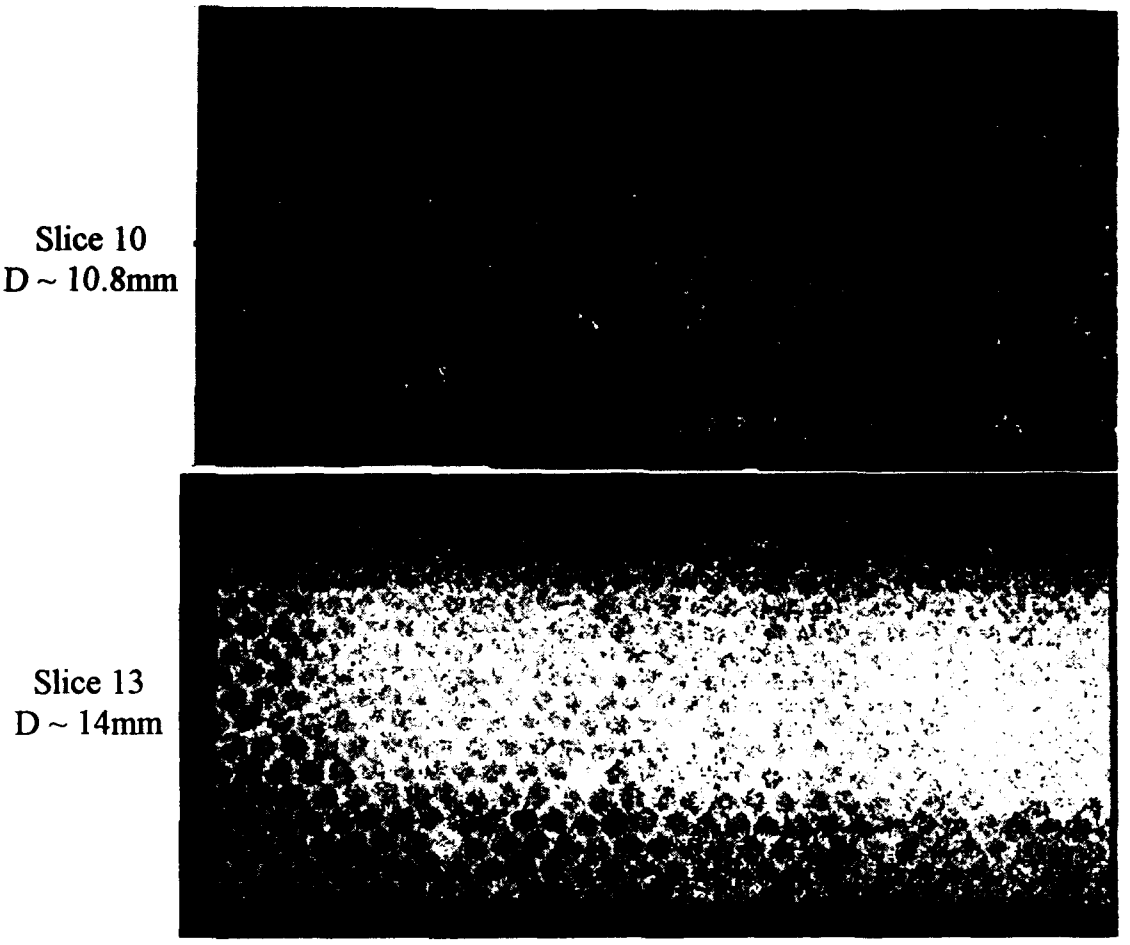

Figure 12. Specimen P1 Grid A.

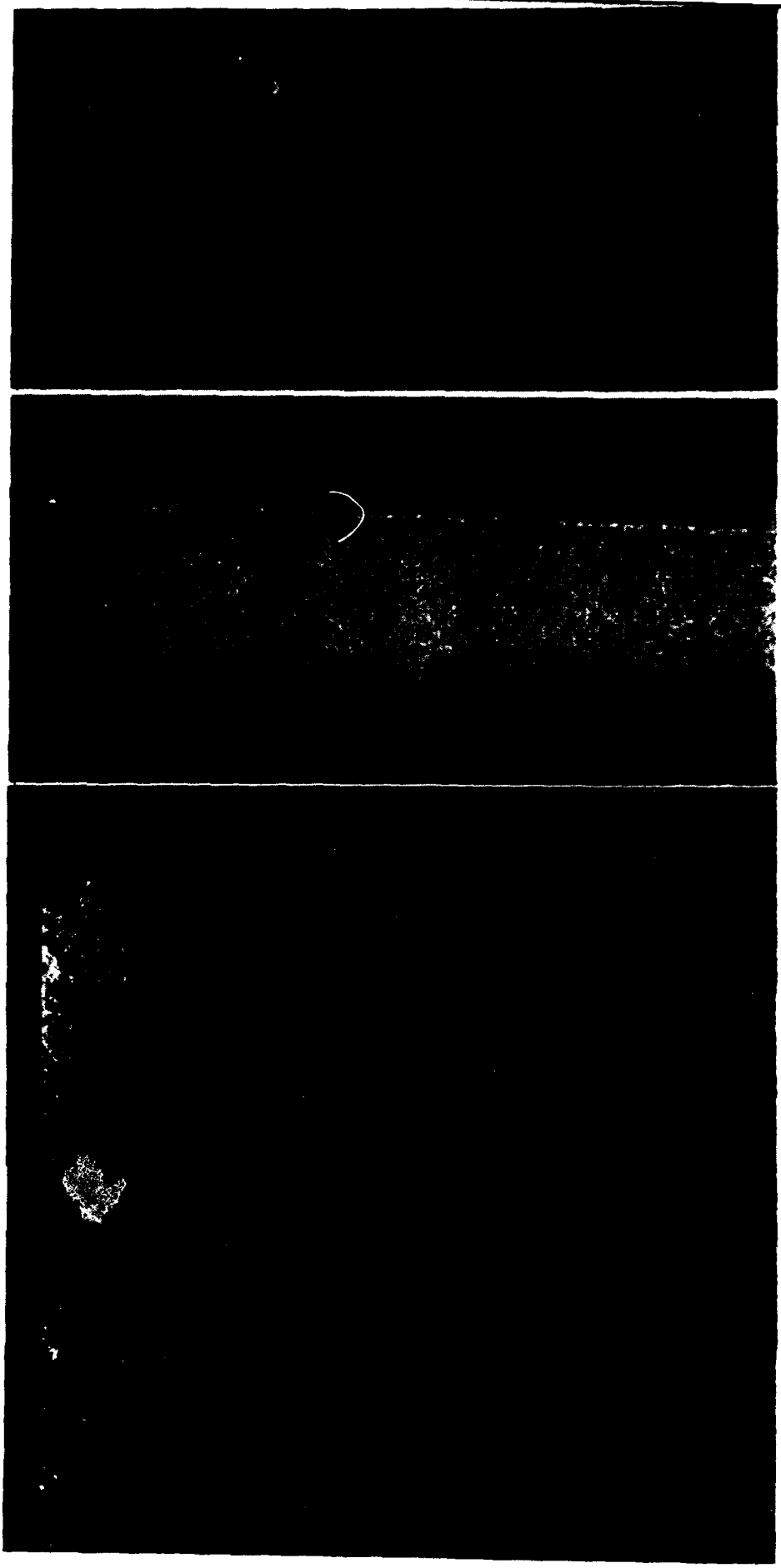

Figure 13. Specimen P1 Grid D.

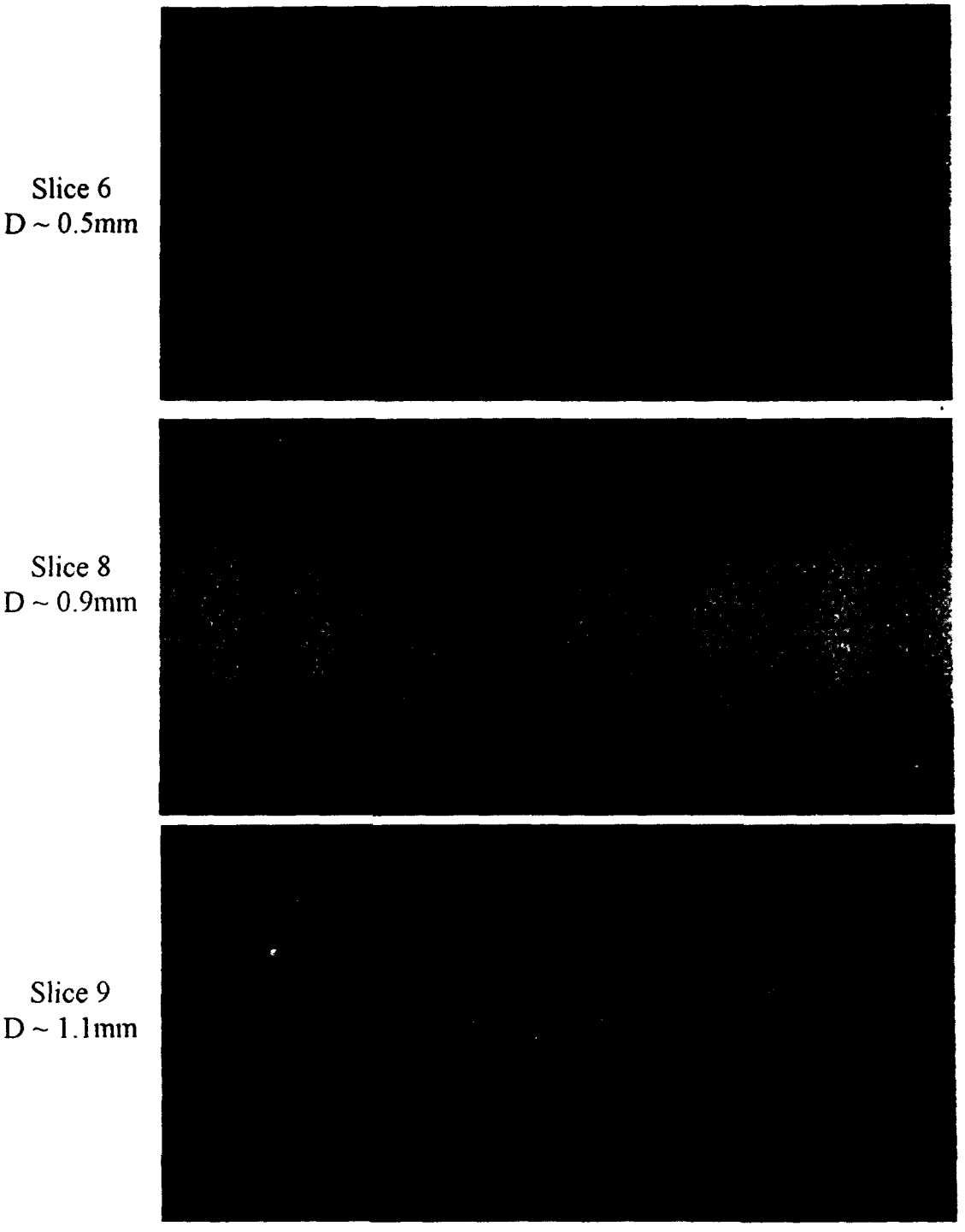

Figure 14. Specimen P1 Grid E.

Slice 11
D ~ 13mm

Slice 12
D ~ 13.5mm

Slice 17
D ~ 15.8mm

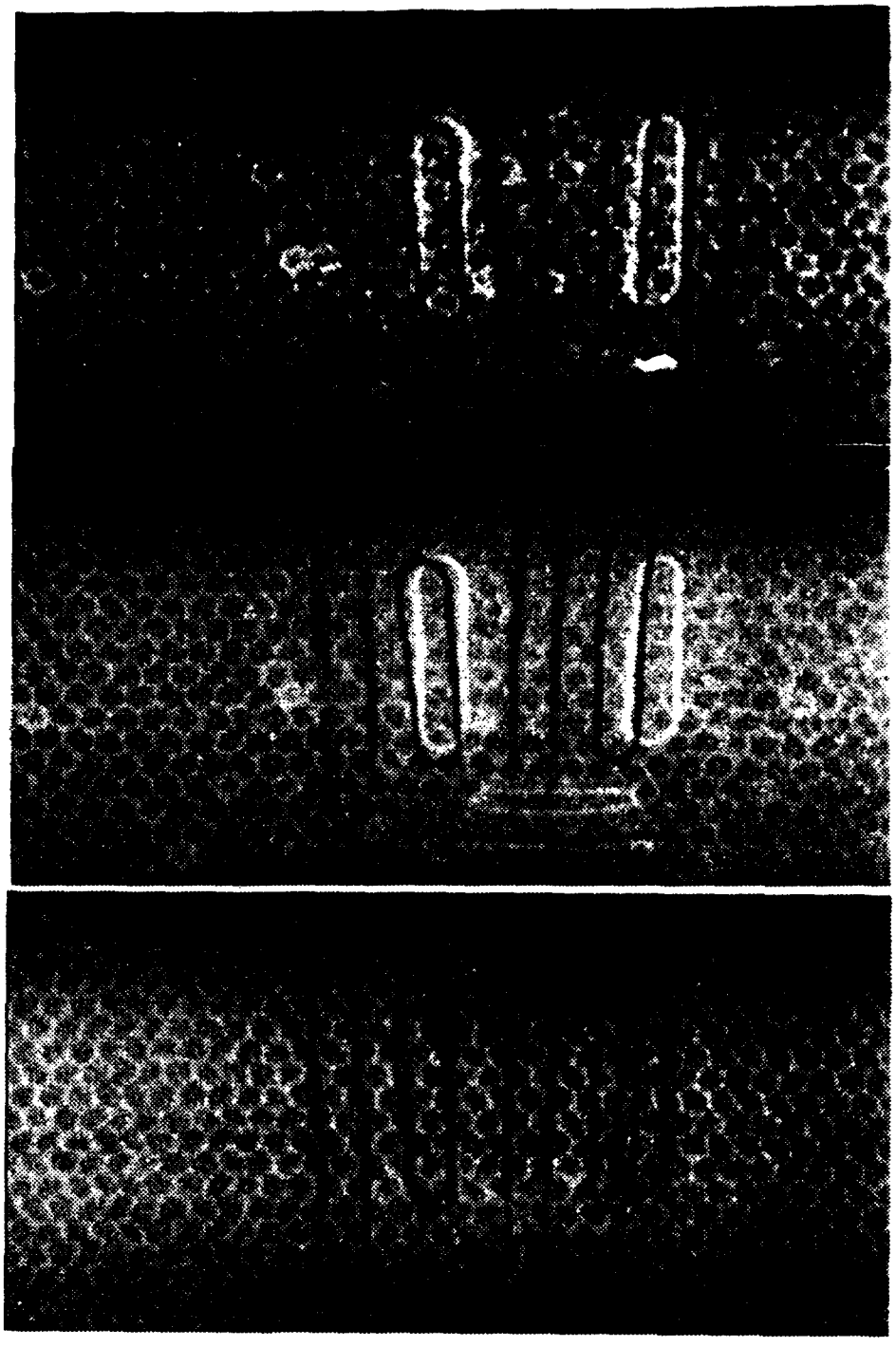

Figure 15. Specimen P1 Grid G/H.

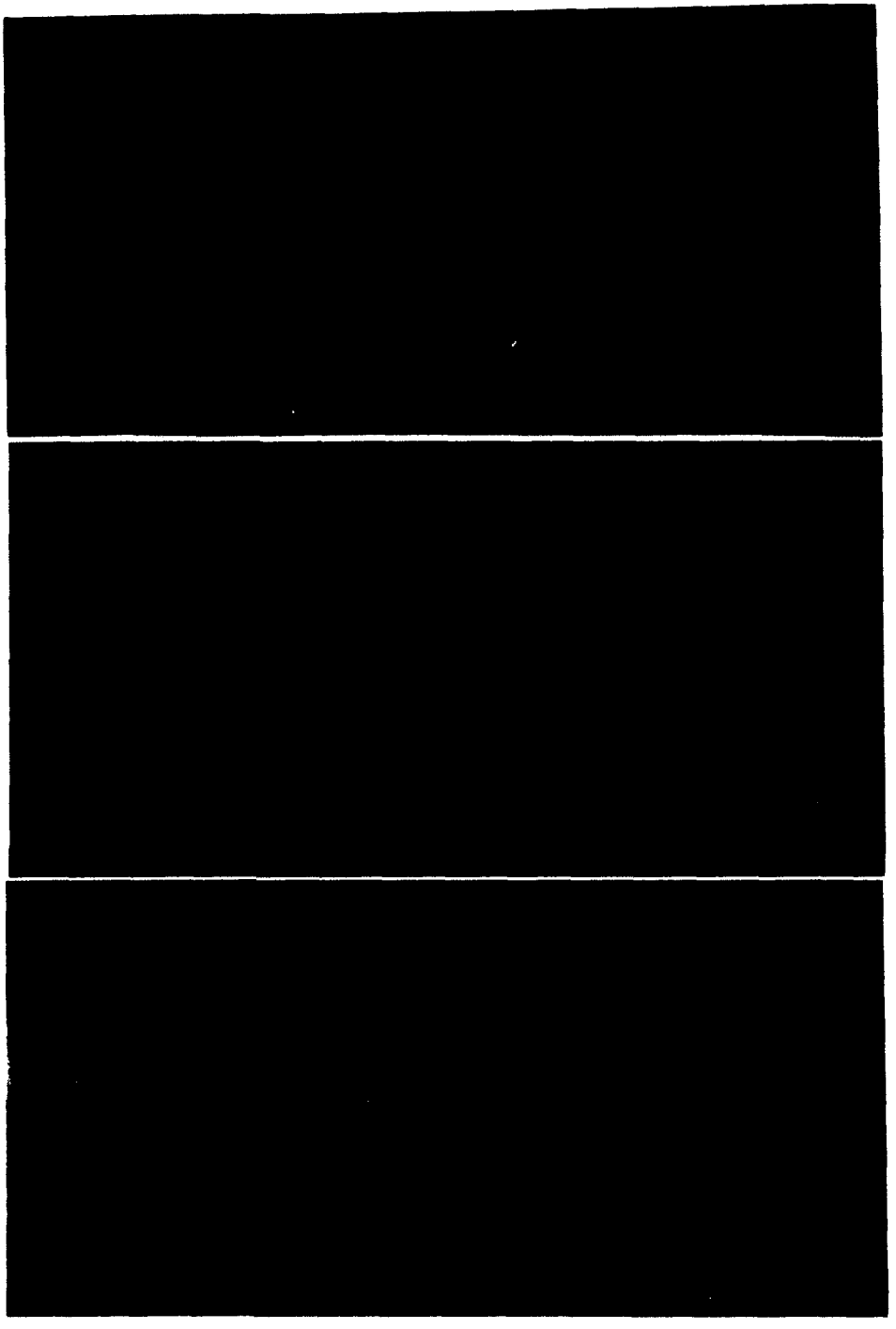

Figure 16. Specimen P1. Grid H.

Slice 9
D ~ 1.6mm

Slice 12
D ~ 2.3mm

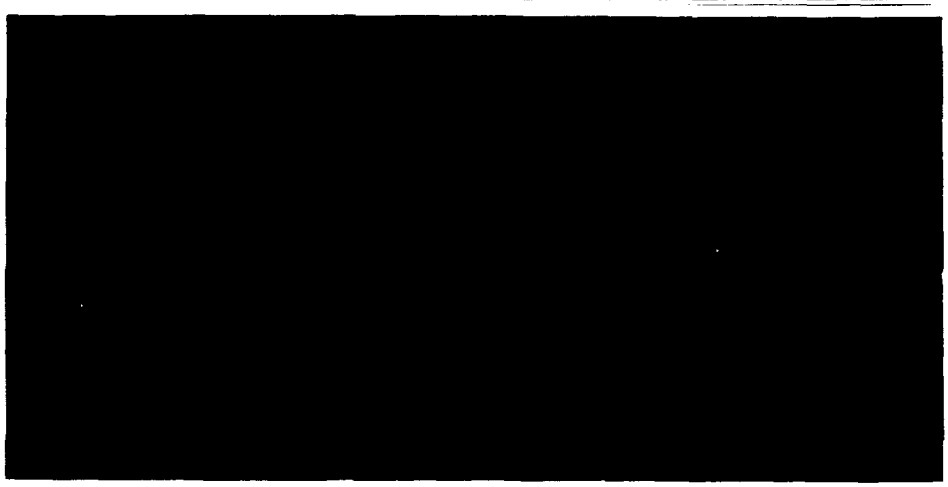

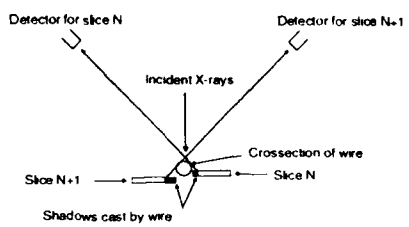

Figure 17. Specimen P1. Grid H.

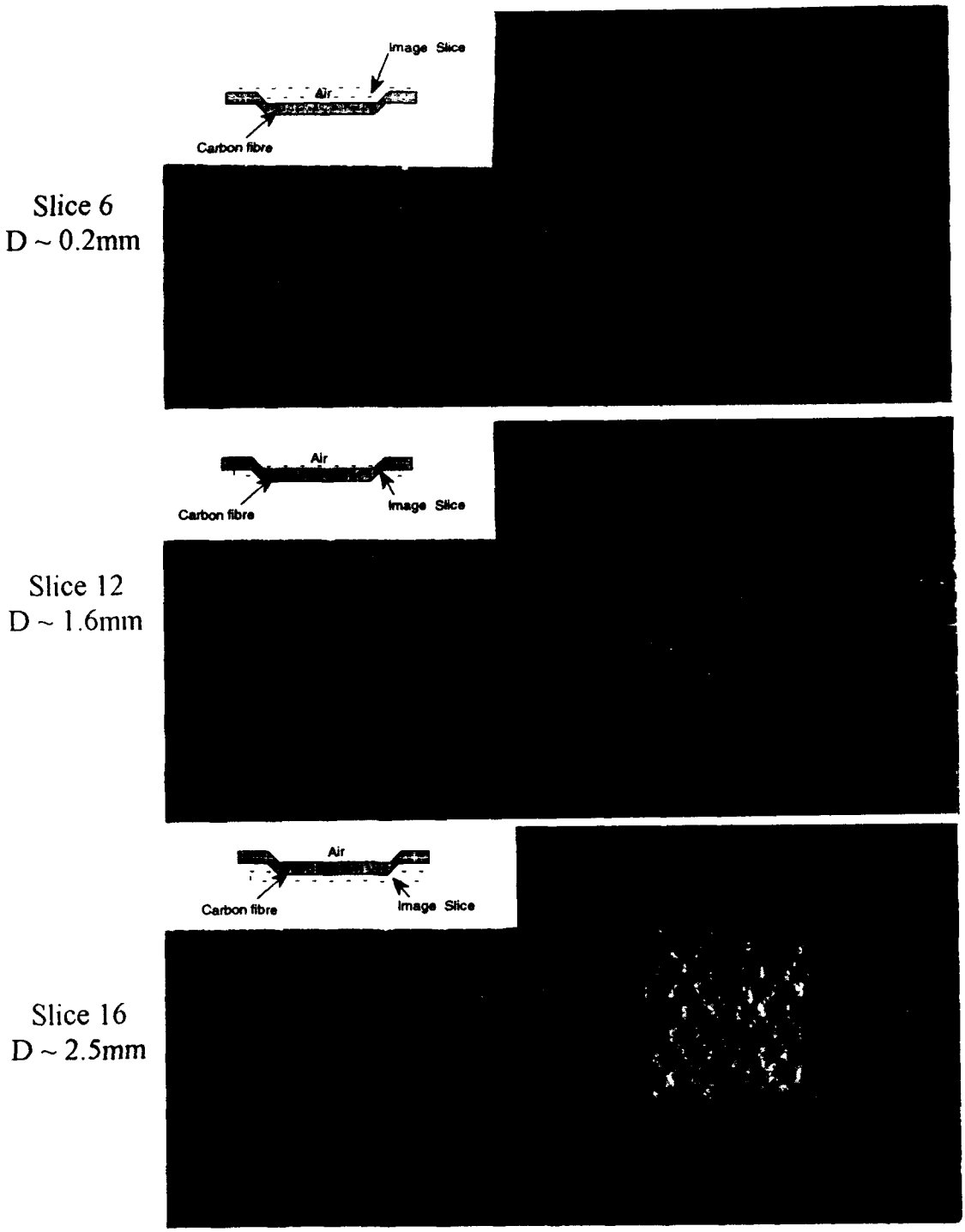

Figure 18 . Specimen P1. Grid I.

Slice 1
D ~ 0mm

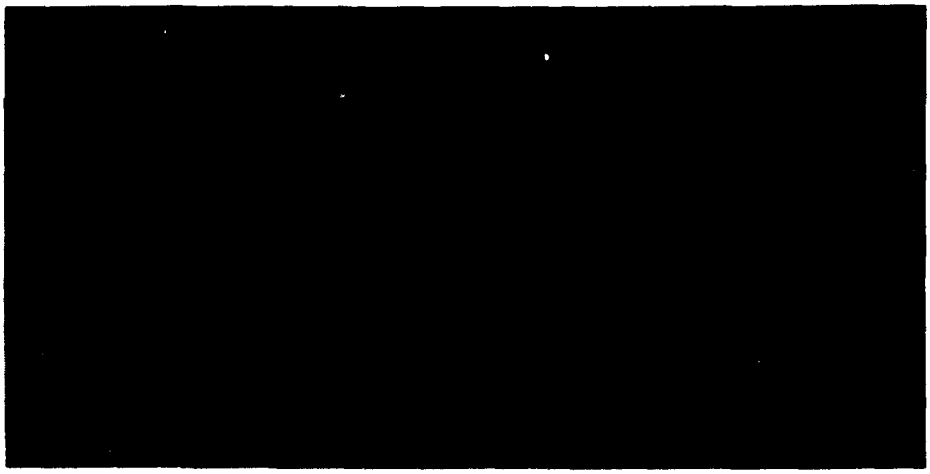

Slice 4
D ~ 0.7mm

Figure 19. Specimen P1. Grid O.

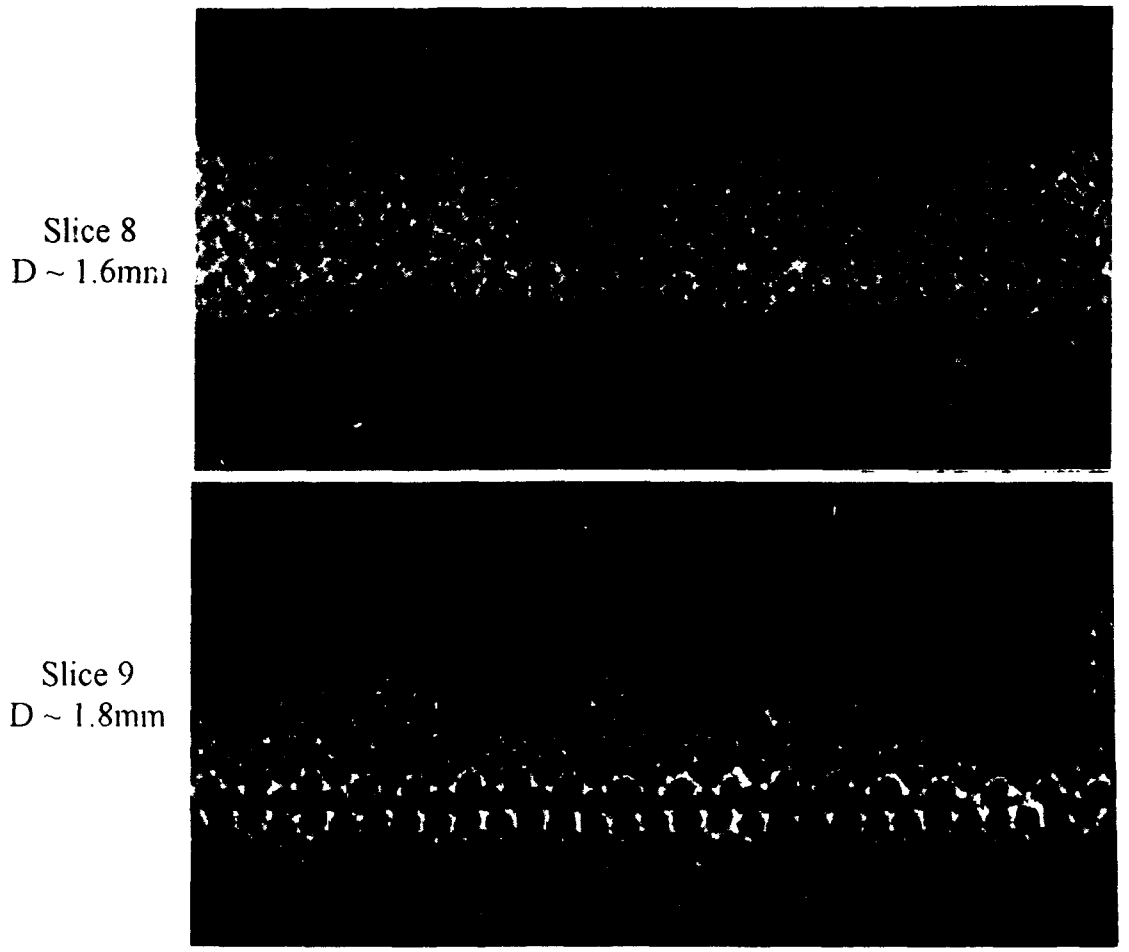

Figure 20. Specimen P1. Grid O.

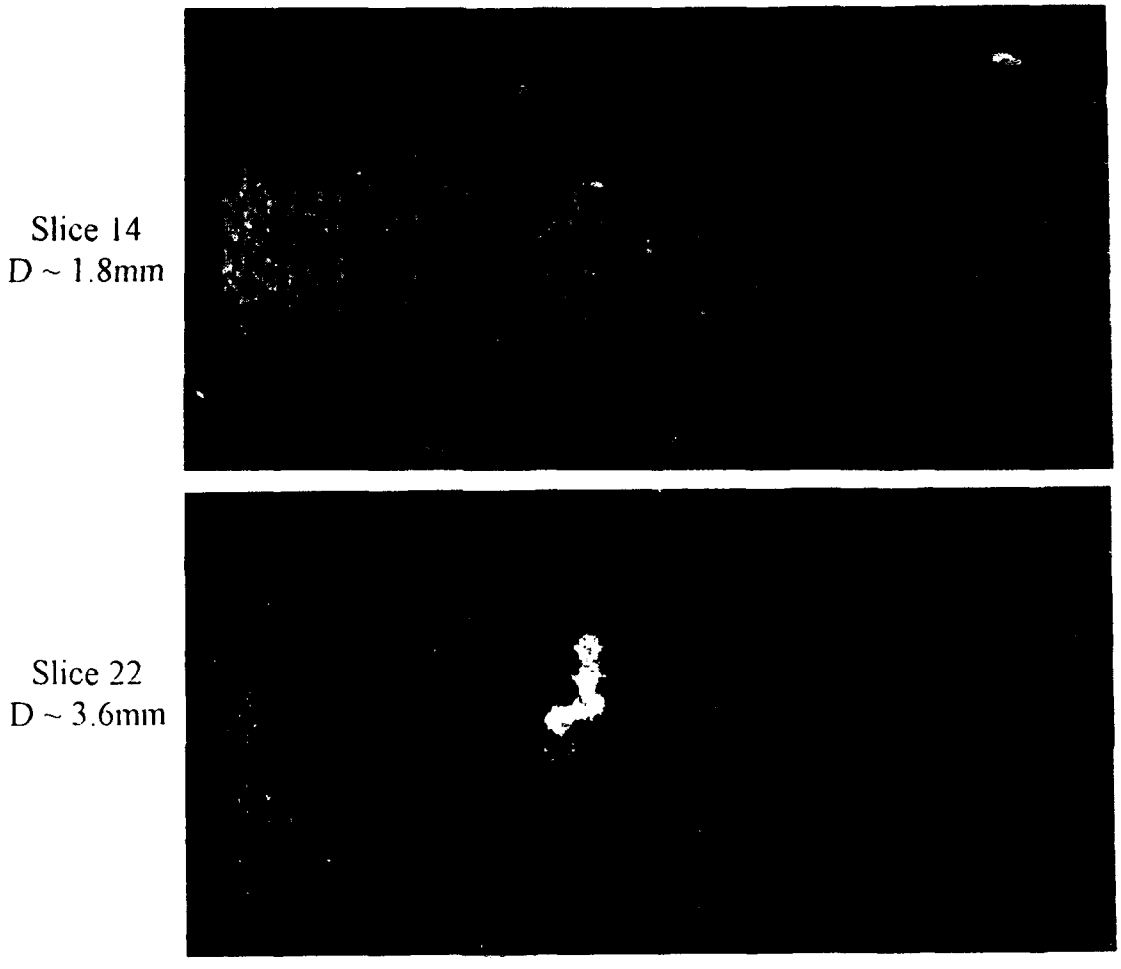

Figure 21. Specimen P1. Grid P.

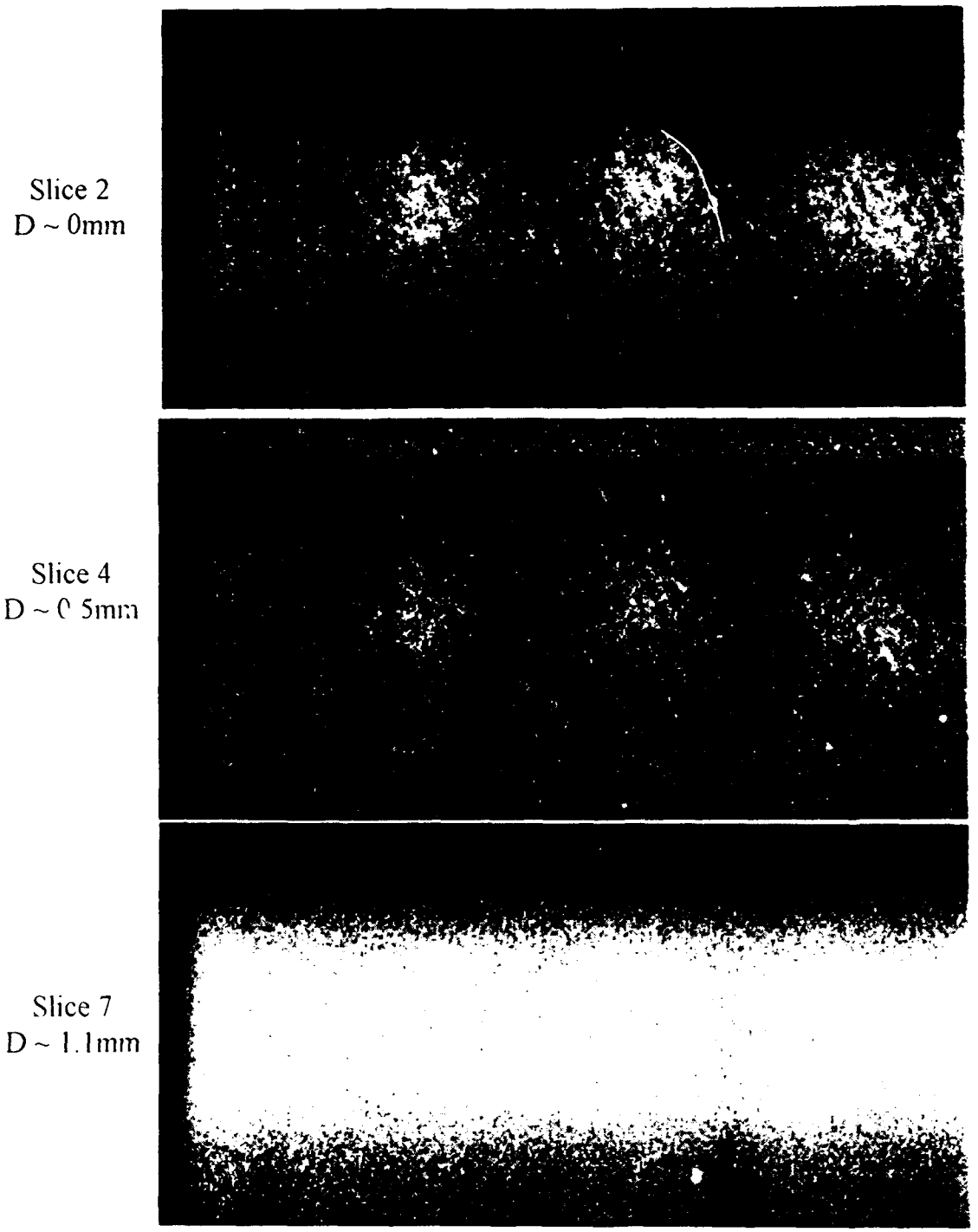

Figure 22. Specimen P2. Grid B.

(a)

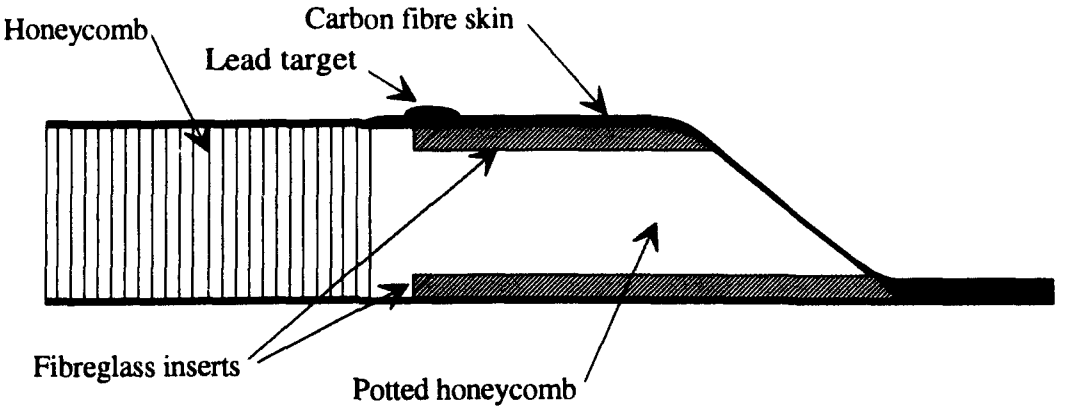

(b) Slice 3
D~3mm

Figure 23. (a) Cross-sectional view of specimen P3.

(b) Image obtained by COMSCAN

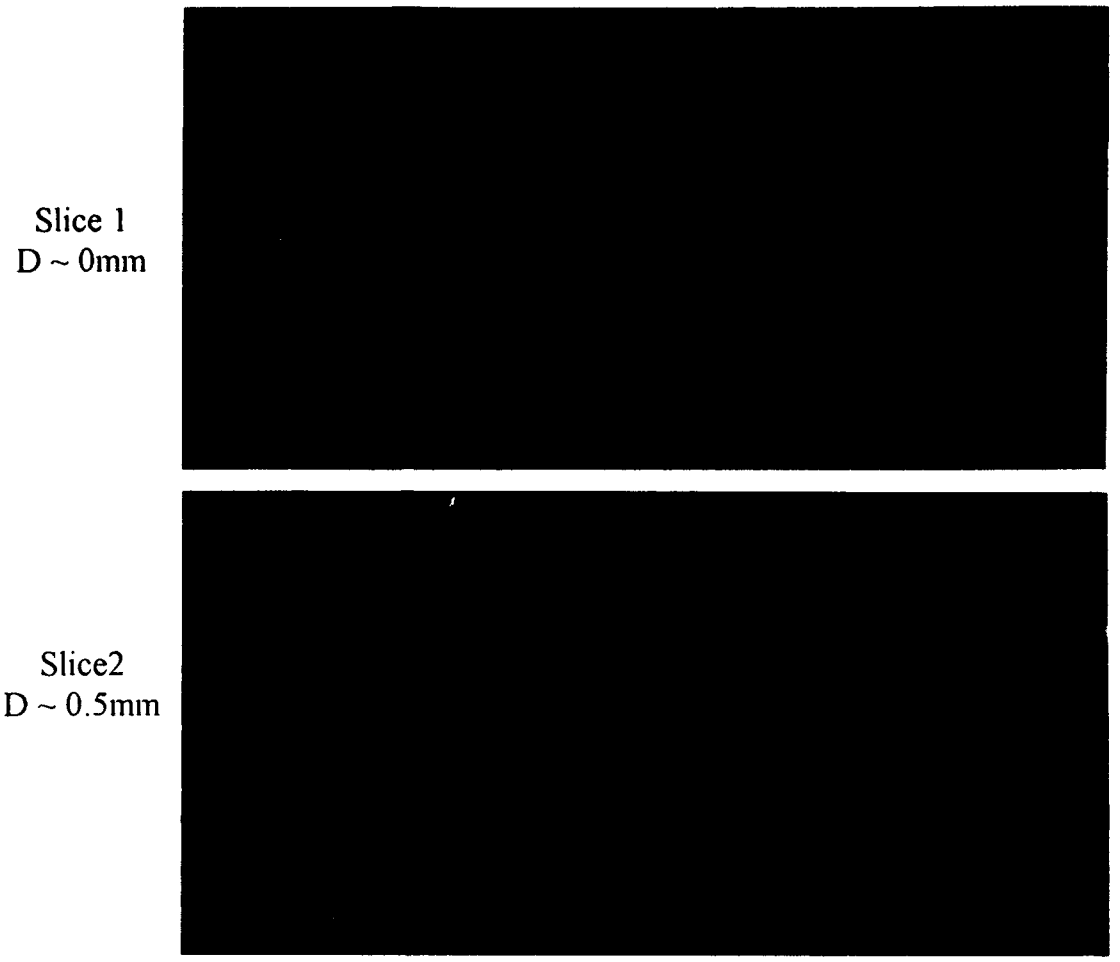

Figure 24. COMSCAN image of coins.

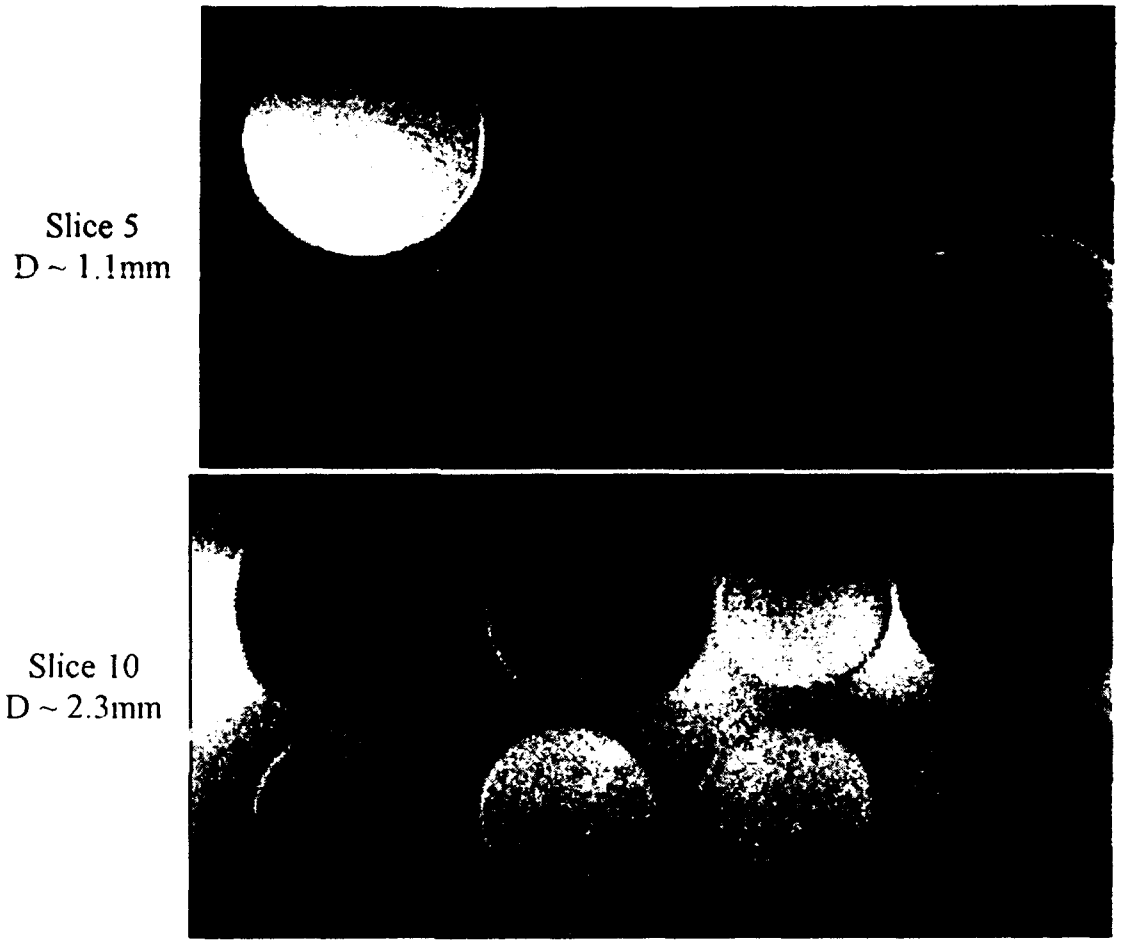

Figure 25. COMSCAN image of coins.

Army

Scientific Adviser - Army (Doc Data sheet only)
Engineering Development Establishment Library
US Army Research, Development and Standardisation Group (3 copies)

Air Force

Air Force Scientific Adviser
Aircraft Research and Development Unit
Scientific Flight Group
Library
PDR AF
DENGPP-AF
AHQ (SMAINTSO)
DGELS (AIRREG4)
OIC NDISL (RAAF Amberley)
503 Wing OIC NDI (RAAF Richmond)
OIC ATF, ATS, RAAFSTT, WAGGA (2 copies)

HQ ADF

Director General Force Development (Air)

Other Organisations

NASA (Canberra)
AGPS
Department of Transport & Communication, Library
ASTA Engineering, Document Control Office
Ansett Airlines of Australia, Library
Australian Airlines, Library
Qantas Airways Limited
Civil Aviation Authority
Hawker de Havilland Aust Pty Ltd, Victoria, Library
Hawker de Havilland Aust Pty Ltd, Bankstown, Library
Rolls Royce of Australia Pty Ltd, Manager
Australian Nuclear Science and Technology Organisation
Gas & Fuel Corporation of Vic., Manager Scientific Services
SEC of Vic., Herman Research Laboratory, Library
BHP, Melbourne Research Laboratories

CANADA

Defense Research Establishment Pacific
Nondestructive Evaluation Group
Materials Technology Section
Capt Rick Finlayson
Dr William Sturrock
K.K. Yeung

SPARES (6 COPIES)

TOTAL (75 COPIES)

DISTRIBUTION

AUSTRALIA

Defence Organisation

Defence Central

Chief Defence Scientist
AS, Science Corporate Management } shared copy
FAS Science Policy
Counsellor, Defence Science, London (Doc Data sheet only)
Counsellor, Defence Science, Washington (Doc Data sheet only)
Scientific Adviser, Defence Central
OIC TRS, Defence Central Library
Document Exchange Centre, DSTIC (8 copies)
Defence Intelligence Organisation
Librarian, Defence Signals Directorate, (Doc Data sheet only)
S.A. to Thailand MRD (Doc Data sheet only)
S.A. to the DRC (Kuala Lumpur) (Doc Data sheet only)
Director General - Army Development (NSO) (4 copies)
Industry Policy and Programs Branch, FAS

Aeronautical Research Laboratory

Director
Library
Chief Airframes and Engines Division
Author: Leo Sponder
S. Burke
A. Baker
G. Clark
G. Long (CRC)

Materials Research Laboratory

P. Lambrineas
R. Woodwood
B. Suendermann

Defence Science & Technology Organisation - Salisbury

Library

Navy

Navy Scientific Adviser (3 copies Doc Data sheet only)
Aircraft Maintenance and Flight Trials Unit
RAN Tactical School, Library
Director Aircraft Engineering - Navy
Director of Naval Architecture
Naval Support Command
Superintendent, Naval Aircraft Logistics
Directorate of Aviation Projects - Navy

AL 149 DEPARTMENT OF DEFENCE

DOCUMENT CONTROL DATA

PAGE CLASSIFICATION
UNCLASSIFIED

PRIVACY MARKING

1a. AR NUMBER	1b. ESTABLISHMENT NUMBER	2. DOCUMENT DATE	3. TASK NUMBER
AR-008-346	ARL-TR-34	JULY 1993	AIR 92/199

4. TITLE
AN ASSESSMENT OF COMSCAN, A COMPTON BACKSCATTER IMAGING CAMERA, FOR THE ONE-SIDED NON-DESTRUCTIVE INSPECTION OF AEROSPACE COMPONENTS

5. SECURITY CLASSIFICATION (PLACE APPROPRIATE CLASSIFICATION IN BOX(S) IE. SECRET (S), CONF. (C) RESTRICTED (R), LIMITED (L), UNCLASSIFIED (U)).

DOCUMENT	TITLE	ABSTRACT
U	U	U

6. NO. PAGES
41

7. NO. REFS.
5

8. AUTHOR(S)
L. SPONDER

9. DOWNGRADING/DELIMITING INSTRUCTIONS
Not applicable.

10. CORPORATE AUTHOR AND ADDRESS

AERONAUTICAL RESEARCH LABORATORY

AIRFRAMES AND ENGINES DIVISION

506 LORIMER STREET

FISHERMENS BEND VIC 3207

11. OFFICE/POSITION RESPONSIBLE FOR:

SPONSOR RAAF OIC NDISL

SECURITY -

DOWNGRADING -

APPROVAL CAED

12. SECONDARY DISTRIBUTION (OF THIS DOCUMENT)

Approved for public release.

OVERSEAS ENQUIRIES OUTSIDE STATED LIMITATIONS SHOULD BE REFERRED THROUGH DSTIC, ADMINISTRATIVE SERVICES BRANCH, DEPARTMENT OF DEFENCE, ANZAC PARK WEST OFFICES, ACT 2601

13a. THIS DOCUMENT MAY BE ANNOUNCED IN CATALOGUES AND AWARENESS SERVICES AVAILABLE TO ....
No limitations

13b. CITATION FOR OTHER PURPOSES (IE. CASUAL ANNOUNCEMENT) MAY BE [X] UNRESTRICTED OR [ ] AS FOR 13a.

14. DESCRIPTORS
Aircraft components
Spacecraft components
Nondestructive tests
X ray inspection
Cameras
Compton effect

15. DISCAT SUBJECT CATEGORIES
140201
0103

16. ABSTRACT

This report presents some results obtained using a Compton backscatter imaging camera, developed by Philips Industries, which were obtained during a visit to the Defense Research Establishment Pacific (DREP) during May/June 1992. Compton backscatter imaging is an X-ray technique which can be used to non-destructively inspect the interior of both metallic and non-metallic structures and, unlike conventional X-ray methods, requires access to only one side of the part being inspected.

PAGE CLASSIFICATION
UNCLASSIFIED
PRIVACY MARKING

THIS PAGE IS TO BE USED TO RECORD INFORMATION WHICH IS REQUIRED BY THE ESTABLISHMENT FOR ITS OWN USE BUT WHICH WILL NOT BE ADDED TO THE DISTS DATA UNLESS SPECIFICALLY REQUESTED.

16. ABSTRACT (CONT).

17. IMPRINT

AERONAUTICAL RESEARCH LABORATORY, MELBOURNE

18. DOCUMENT SERIES AND NUMBER	19. WA NUMBER	20. TYPE OF REPORT AND PERIOD COVERED
Technical Report 34	31 340C	

21. COMPUTER PROGRAMS USED

22. ESTABLISHMENT FILE REF.(S)

23. ADDITIONAL INFORMATION (AS REQUIRED)